AIMS Mathematics, 8(6): 14207–14231.
DOI: 10.3934/math.2023727
Received: 06 January 2023
Revised: 01 April 2023
Accepted: 03 April 2023
Published: 17 April 2023

http://www.aimspress.com/journal/Math

Research article

A multigrid discretization scheme of discontinuous Galerkin method for the Steklov-Lamé eigenproblem

Liangkun Xu and Hai Bi*

School of Mathematical Sciences, Guizhou Normal University, Universities Town, Huaxi District, Guiyang, Guizhou, China

* **Correspondence:** Email: bihaimath@gznu.edu.cn; Tel: +8685183227512.

Abstract: In this paper, for the Steklov-Lamé eigenvalue problem, we propose a multigrid discretization scheme of discontinuous Galerkin method based on the shifted-inverse iteration. Based on the existing a priori error estimates, we give the error estimates for the proposed scheme and prove that the resulting approximations can achieve the optimal convergence order when the mesh sizes fit into some relationships. Finally, we combine the multigrid scheme and adaptive procedure to present some numerical examples which indicate that our scheme are locking-free and efficient for computing Steklov-Lamé eigenvalues.

Keywords: Steklov-Lamé eigenvalues; discontinuous finite element; multigrid discretization; shifted-inverse iteration; adaptive computation
Mathematics Subject Classification: 65N25, 65N30

1. Introduction

The Steklov spectrum coincides with that of the Dirichlet-to-Neumann map for the Laplacian (see, e.g., [1]), and the Steklov eigenvalue problem for the Laplace operator has been well-studied in the mathematical community. In linear elasticity, the study of the Dirichlet-to-Neumann map is important in elastostatic problems, and has attracted the attention of scholars (see, e.g., [2–4]). In 2021, Domínguez [5] first introduced the Steklov-Lamé eigenvalue problem in which the spectral parameter appears on a Robin boundary condition. [5] investigated the existence of the countable spectrum of this problem and studied the conforming finite element methods for the Steklov Lamé problem. Later, Li and Bi [6] proposed a discontinuous finite element method for this problem and gave the a priori error estimates.

As we know, for numerical solutions of the problems in linear planar elasticity, standard conforming finite elements may suffer a deterioration in performance as the Lam*é* constant $\lambda \to \infty$,

that is locking phenomenon (see [7, 8]). To overcome the locking phenomenon, several numerical approaches have been developed including the p-version method [9], the PEERS method [10], the mixed method [11], the Galerkin least squares method [12], the nonconforming triangular elements [13, 14] and the discontinuous finite element method [15–17], and so on.

On the other hand, based on standard finite element methods, people design many efficient discretization schemes/algorithms to get approximations with high accuracy or to reduce the computation costs. The finite element multigrid discretizations is one of such design approaches. This method benefits from the two-grid discretization scheme which was first proposed by Xu and Zhou [18, 19]. The basic idea of the two-grid discretizations is to transform solving an eigenvalue problem on a fine grid into solving the eigenvalue problem on a coarse grid and solving a series of algebraic equations on the fine grid. This kind of method can save calculation time while keeping the accuracy of approximations, or improving the accuracy under the same degrees of freedom. So far, two-grid and multigrid finite element discretization schemes have been successfully applied to solving eigenvalue problems, such as elliptic eigenvalue problem [20], Steklov eigenvalue problem [21–24], biharmonic eigenvalue problem [25], semilinear elliptic eigenvalue problem [26], quantum eigenvalue problem [27], Stokes eigenvalue problem [28, 29], Maxwell eigenvalue problem [30], $2m$-order elliptic eigenvalue problem [31], etc.

At present, there is not much numerical research report on the Steklov-Lamé eigenproblem. In view of the characteristics of discontinuous finite element method (DGFEM) and multigrid discretizations and based on the work in [6, 32], for the Steklov-Lamé eigenvalue problem we will design and analyze a multigrid discretization scheme of DGFEM based on the shifted-inverse iteration. The rest of this paper is organized as follows. In Section 2, the discontinuous finite element approximation of the Steklov-Lamé eigenvalue problem and its a prior error estimates are given. In Section 3, a multigrid discretization scheme of DGFEM based on the shifted-inverse iteration is established, and the error estimates of the proposed scheme is presented. Finally, in Section 4, an adaptive multigrid algorithm is provided coupled with some numerical experiment results. The numerical results show that our method is efficient and locking-free.

Before the discussion, let us specify some notations. Scalars are denoted by general letters, vectors are denoted by bold letters and tensors in bold Greek letters. For tensors $\boldsymbol{\sigma}, \boldsymbol{\tau} \in \mathbb{R}^{n\times n}$, the double dot product notation $\boldsymbol{\sigma} : \boldsymbol{\tau} = tr(\boldsymbol{\tau}^T\boldsymbol{\sigma})$ where $tr(\cdot)$ denotes the trace of a tensor (sum of the main diagonal). This inner product induces the Frobenius norm for tensors which is denoted as $\|\cdot\|$. Let $H^s(\Omega)$ and $H^s(\partial\Omega)$ be the usual Sobolev space with order s of scalar fields on Ω and $\partial\Omega$, respectively, whereas for tensor fields we use the symbols $\boldsymbol{H}^s(\Omega)$ and $\boldsymbol{H}^s(\partial\Omega)$ and each element in $\boldsymbol{H}^s$ belongs to H^s. The norm in $H^s(\Omega)$ and $H^s(\partial\Omega)$ are denoted by $\|\cdot\|_s$ and $\|\cdot\|_{s,\partial\Omega}$, respectively, and the same symbols are also used for the norms in $\boldsymbol{H}^s(\Omega)$ and $\boldsymbol{H}^s(\partial\Omega)$ when there is no ambiguity. $H^0(\partial\Omega) = L^2(\partial\Omega)$. Throughout this paper, we use the letter C, with or without subscript, to denote a generic positive constant independent of the mesh size h and the Lamé parameters, which may not be the same at each occurrence. We use the symbol $a \lesssim b$ to mean that $a \leq Cb$.

2. DGFEM approximation of the Steklov-Lamé eigenproblem

Suppose that an isotropic and linearly elastic material occupies the region Ω in $\mathbb{R}^n$ ($n = 2$ *or* 3) where Ω is a bounded convex polygonal with Lipschitz continuous boundary $\partial\Omega$. Consider the following

Steklov-Lamé eigenvalue problem: Find non-zero displacement vector $\boldsymbol{u}$ and the frequencies $\omega \in \mathbb{R}$ satisfying

$$\begin{cases} -div\boldsymbol{\sigma}(\boldsymbol{u}) = \mathbf{0} & in\ \Omega, \\ \boldsymbol{\sigma}(\boldsymbol{u})\boldsymbol{n} = \omega p\boldsymbol{u} & on\ \partial\Omega, \end{cases} \tag{2.1}$$

where $\boldsymbol{n}$ is the unit outward normal to $\partial\Omega$, $\boldsymbol{\sigma}(\boldsymbol{u})$ is the Cauchy stress tensor defined as

$$\boldsymbol{\sigma}(\boldsymbol{u}) = 2\mu\boldsymbol{\epsilon}(\boldsymbol{u}) + \lambda tr(\boldsymbol{\epsilon}(\boldsymbol{u}))\boldsymbol{I},$$

where $\boldsymbol{I} \in \mathbb{R}^{n\times n}$ is the identity matrix, $\boldsymbol{\epsilon}(\boldsymbol{u})$ is the strain tensor given by

$$\boldsymbol{\epsilon}(\boldsymbol{u}) = \frac{1}{2}\left(\nabla\boldsymbol{u} + (\nabla\boldsymbol{u})^T\right),$$

$\nabla\boldsymbol{u}$ is the displacement gradient tensor, and $\lambda \in \mathbb{R}$ and $\mu > 0$ are the Lamé parameters satisfying $0 < \mu_1 < \mu < \mu_2$ and $0 < \lambda < \infty$.

Suppose that the density of material $p \in L^\infty(\partial\Omega)$ has positive lower bound on $\partial\Omega$.

Denote

$$\mathbf{RM}(\Omega) := \{\boldsymbol{v} \in \boldsymbol{H}^1(\Omega) | \boldsymbol{v}(\boldsymbol{x}) = \boldsymbol{a} + \boldsymbol{B}\boldsymbol{x}, \boldsymbol{a} \in \mathbb{R}^n, \boldsymbol{B} \in \mathbb{R}^{n\times n}, \boldsymbol{B}^T = -\boldsymbol{B}, \boldsymbol{x} \in \Omega\}.$$

It is obvious that 0 is an eigenvalue of (2.1) with the associated eigenfunction $\boldsymbol{u} \in \mathbf{RM}(\Omega)$ (see [5]). To find non-zero eigenvalues of (2.1), we adopt the following weak formulation: Seek $(\kappa, \boldsymbol{u}) \in \mathbb{R} \times \boldsymbol{H}^1(\Omega)$ such that

$$a(\boldsymbol{u}, \boldsymbol{v}) = \kappa b(\boldsymbol{u}, \boldsymbol{v}),\ \forall \boldsymbol{v} \in \boldsymbol{H}^1(\Omega), \tag{2.2}$$

where $\kappa = \omega + 1$,

$$\begin{aligned} a(\boldsymbol{u}, \boldsymbol{v}) &:= \int_\Omega \boldsymbol{\sigma}(\boldsymbol{u}) : \boldsymbol{\epsilon}(\boldsymbol{v})dx + \int_{\partial\Omega} p\boldsymbol{u} \cdot \boldsymbol{v}ds \\ &= 2\mu \int_\Omega \boldsymbol{\epsilon}(\boldsymbol{u}) : \boldsymbol{\epsilon}(\boldsymbol{v})dx + \lambda \int_\Omega (div\boldsymbol{u})(div\boldsymbol{v})dx + \int_{\partial\Omega} p\boldsymbol{u} \cdot \boldsymbol{v}ds,\ \forall \boldsymbol{u}, \boldsymbol{v} \in \boldsymbol{H}^1(\Omega), \\ b(\boldsymbol{u}, \boldsymbol{v}) &:= \int_{\partial\Omega} p\boldsymbol{u} \cdot \boldsymbol{v}ds,\ \forall \boldsymbol{u}, \boldsymbol{v} \in \boldsymbol{H}^1(\Omega). \end{aligned}$$

Reference [5] proved that $a(\cdot,\cdot)$ is a continuous and $\boldsymbol{H}^1$-coercive bilinear form in $\boldsymbol{H}^1(\Omega)$, $b(\cdot,\cdot)$ is bounded.

Without losing generality, we assume that $p \equiv 1$ in the rest of this paper. Denote $\|\boldsymbol{v}\|_b = b(\boldsymbol{v}, \boldsymbol{v})^{\frac{1}{2}}$, then it is clear that $\|\cdot\|_b = \|\cdot\|_{0,\partial\Omega}$.

Let $\mathcal{T}_h = \{K\}$ be a shape-regular partition of Ω, and $h = \max\{h_K : K \in \mathcal{T}_h\}$ is the diameter of $\mathcal{T}_h$ where h_K is the diameter of element K. When $n = 2$, K is a triangle and a tetrahedron when $n = 3$. Let $e \in \partial K$ be an edge/face of element K with diameter h_e, and let $\Gamma_h = \Gamma_h^i \cup \Gamma_h^b$ where Γ_h^i denotes the interior edges/faces set and Γ_h^b denotes the set of edges/faces lying on the boundary $\partial\Omega$. In the following, when there is no confusion we always use $\boldsymbol{n}$ to represent the unit outward normal on the boundary of Ω or element K.

Define the broken Sobolev space:

$$\boldsymbol{H}^s(\mathcal{T}_h) = \{\boldsymbol{v} \in [L_2(\Omega)]^n : \boldsymbol{v}\,|_K \in [H^s(K)]^n, \forall K \in \mathcal{T}_h\}.$$

For any $\boldsymbol{v} \in \boldsymbol{H}^s(\mathcal{T}_h)$, define the jump $[\![\boldsymbol{v}]\!]$ and the average $\{\boldsymbol{v}\}$ on e as follows:

$$[\![\boldsymbol{v}]\!] = \begin{cases} \boldsymbol{v}^+ - \boldsymbol{v}^-, & e \in \Gamma_h^i, \\ \boldsymbol{v}^+ \quad\;\; , & e \in \Gamma_h^b, \end{cases} \qquad \{\boldsymbol{v}\} = \begin{cases} \frac{\boldsymbol{v}^+ + \boldsymbol{v}^-}{2}, & e \in \Gamma_h^i, \\ \boldsymbol{v}^+ \quad , & e \in \Gamma_h^b, \end{cases}$$

where $\boldsymbol{v}^+ = \boldsymbol{v}|_{K^+}, \boldsymbol{v}^- = \boldsymbol{v}|_{K^-}, e \in \partial K^+ \cap \partial K^-$.

Define the DGFEM space:

$$\boldsymbol{S}^h = \{\boldsymbol{v} \in [L_2(\Omega)]^n : \boldsymbol{v}\,|_K \in [\mathcal{P}^k(K)]^n, \forall K \in \mathcal{T}_h\},$$

where $\mathcal{P}^k(K)$ is the space of polynomials defined on K with degree less than or equal to $k \geq 1$.

The DGFEM discretization for the problem (2.2) is to find $(\kappa_h, \boldsymbol{u}_h) \in \mathbb{R} \times \boldsymbol{S}^h, \boldsymbol{u}_h \neq 0, \kappa_h = \omega_h + 1$, such that

$$a_h(\boldsymbol{u}_h, \boldsymbol{v}_h) = \kappa_h b_h(\boldsymbol{u}_h, \boldsymbol{v}_h), \;\; \forall \boldsymbol{v}_h \in \boldsymbol{S}^h, \tag{2.3}$$

where

$$\begin{aligned} a_h(\boldsymbol{u}_h, \boldsymbol{v}_h) \;=\; & 2\mu \Bigg(\sum_{K \in \mathcal{T}_h} \int_K \boldsymbol{\epsilon}(\boldsymbol{u}_h) : \boldsymbol{\epsilon}(\boldsymbol{v}_h) dx - \sum_{e \in \Gamma_h^i} \int_e \{\boldsymbol{\epsilon}(\boldsymbol{u}_h)\boldsymbol{n}\} \cdot [\![\boldsymbol{v}_h]\!] ds \\ & - \sum_{e \in \Gamma_h^i} \int_e \{\boldsymbol{\epsilon}(\boldsymbol{v}_h)\boldsymbol{n}\} \cdot [\![\boldsymbol{u}_h]\!] ds + \sum_{e \in \Gamma_h^i} \frac{\gamma_\mu}{h_e} \int_e [\![\boldsymbol{u}_h]\!] \cdot [\![\boldsymbol{v}_h]\!] ds \Bigg) \\ & + \lambda \Bigg(\sum_{K \in \mathcal{T}_h} \int_K (div\boldsymbol{u}_h)(div\boldsymbol{v}_h) dx - \sum_{e \in \Gamma_h^i} \int_e \{div\boldsymbol{u}_h\} [\![\boldsymbol{v}_h \cdot \boldsymbol{n}]\!] ds \\ & - \sum_{e \in \Gamma_h^i} \int_e \{div\boldsymbol{v}_h\} [\![\boldsymbol{u}_h \cdot \boldsymbol{n}]\!] ds + \sum_{e \in \Gamma_h^i} \frac{\gamma_\lambda}{h_e} \int_e [\![\boldsymbol{u}_h \cdot \boldsymbol{n}]\!] [\![\boldsymbol{v}_h \cdot \boldsymbol{n}]\!] ds \Bigg) \\ & + \sum_{e \in \Gamma_h^b} \int_e \boldsymbol{u}_h \cdot \boldsymbol{v}_h ds, \\ b_h(\boldsymbol{u}_h, \boldsymbol{v}_h) \;=\; & \sum_{e \in \Gamma_h^b} \int_e \boldsymbol{u}_h \cdot \boldsymbol{v}_h ds, \end{aligned}$$

and the penalty constants $\gamma_\mu, \; \gamma_\lambda$ are independent of the shape of K and h. The determination of γ_μ and γ_λ is to ensure that (2.4) is valid. It is easy to see that the discretization (2.3) is symmetric which is called symmetric internal penalty method (SIPG) in DGFEM.

Define the DG norm:

$$\begin{aligned}\|\boldsymbol{u}_h\|_G^2 &= 2\mu\sum_{K\in\mathcal{T}_h}\|\boldsymbol{\epsilon}(\boldsymbol{u}_h)\|_{0,K}^2+2\mu\sum_{e\in\Gamma_h^i}\gamma_\mu h_e^{-1}\|[\![\boldsymbol{u}_h]\!]\|_{0,e}^2+\lambda\sum_{K\in\mathcal{T}_h}\|div\boldsymbol{u}_h\|_{0,K}^2\\ &+ \lambda\sum_{e\in\Gamma_h^i}\gamma_\lambda h_e^{-1}\|[\![\boldsymbol{u}_h\cdot\boldsymbol{n}]\!]\|_{0,e}^2+\sum_{e\in\Gamma_h^b}\|\boldsymbol{u}_h\|_{0,e}^2,\end{aligned}$$

and the energy-like norm:

$$\|\boldsymbol{u}_h\|_h^2 = \|\boldsymbol{u}_h\|_G^2+2\mu\sum_{e\in\Gamma_h^i}h_e\|\{\boldsymbol{\epsilon}(\boldsymbol{u}_h)\boldsymbol{n}\}\|_{0,e}^2+\lambda\sum_{e\in\Gamma_h^i}h_e\|\{div\boldsymbol{u}_h\}\|_{0,e}^2.$$

From Lemma 4 in [33] we know that there exist constants C_μ and C_λ, independent of h, h_e, μ and λ, such that

$$\begin{aligned}\|h_e^{1/2}\boldsymbol{\epsilon}(\boldsymbol{v})\boldsymbol{n}\|_{0,e}^2 &\le C_\mu\|\boldsymbol{\epsilon}(\boldsymbol{v})\|_{0,K}^2,\\ \|h_e^{1/2}div\boldsymbol{v}\|_{0,e}^2 &\le C_\lambda\|div\boldsymbol{v}\|_{0,K}^2.\end{aligned}$$

Then, for $0<\beta<1$, when $\gamma_\mu \ge C_\mu/(1-\beta)^2$, $\gamma_\lambda \ge C_\lambda/(1-\beta)^2$, the bilinear form $a_h(\cdot,\cdot)$ is coercive on $\boldsymbol{S}^h$ (see Lemma 2.2 in [6]):

$$\beta\|\boldsymbol{v}_h\|_G^2 \le a_h(\boldsymbol{v}_h,\boldsymbol{v}_h), \quad \forall\boldsymbol{v}_h\in\boldsymbol{S}^h. \tag{2.4}$$

Using Cauchy-Schwartz inequality, it is easy to prove that the bilinear form $a_h(\cdot,\cdot)$ is continuous:

$$|a_h(\boldsymbol{u},\boldsymbol{v})| \le M\|\boldsymbol{u}\|_h\|\boldsymbol{v}\|_h, \quad \forall\boldsymbol{u},\boldsymbol{v}\in\boldsymbol{H}^{1+s}(\mathcal{T}_h), s>\frac{1}{2}.$$

In order to derive the convergence and the error estimates of DG approximations by using Babuška-Osborn spectral approximation theory, we consider the following source problem associated with the eigenvalue problem (2.2): find $\boldsymbol{w}\in\boldsymbol{H}^1(\Omega)$ such that

$$a(\boldsymbol{w},\boldsymbol{v}) = b(\boldsymbol{f},\boldsymbol{v}),\ \forall\boldsymbol{v}\in\boldsymbol{H}^1(\Omega). \tag{2.5}$$

The DG approximation of (2.5) is to find $\boldsymbol{w}_h\in\boldsymbol{S}^h$ such that

$$a_h(\boldsymbol{w}_h,\boldsymbol{v}_h) = b_h(\boldsymbol{f},\boldsymbol{v}_h),\ \forall\boldsymbol{v}_h\in\boldsymbol{S}^h. \tag{2.6}$$

Since $a(\cdot,\cdot)$ and $a_h(\cdot,\cdot)$ are continuous and coercive on $\boldsymbol{H}^1(\Omega)$ and $\boldsymbol{S}^h$, respectively, $b(\cdot,\cdot)$ and $b_h(\cdot,\cdot)$ are bounded, from Lax-Milgram Theorem we know that (2.5) and (2.6) admit the unique solution $\boldsymbol{w}$ and $\boldsymbol{w}_h$, respectively.

The following regularity estimates of the solution of (2.5) has been discussed in Lemma 3.1 of [6].

(1) Let $\boldsymbol{w}$ be the solution of (2.5). If $\boldsymbol{f}\in\boldsymbol{H}^{r-\frac{1}{2}}(\partial\Omega)$, then $\boldsymbol{w}\in\boldsymbol{H}^{r+1}(\Omega)$ and

$$\|\boldsymbol{w}\|_{r+1}+\lambda\|div\boldsymbol{w}\|_r \le C_R\|\boldsymbol{f}\|_{r-\frac{1}{2},\partial\Omega},$$

where $r=1$ when Ω is a convex polygonal, and r can be large enough when $\partial\Omega$ is sufficiently smooth;

(2) If $\boldsymbol{f}\in\boldsymbol{H}^{-\frac{1}{2}}(\partial\Omega)$, then $\boldsymbol{w}\in\boldsymbol{H}^1(\Omega)$ and

$$\|\boldsymbol{w}\|_1+\lambda\|div\boldsymbol{w}\|_0 \le C_R\|\boldsymbol{f}\|_{-\frac{1}{2},\partial\Omega};$$

(3) If $\boldsymbol{f} \in \boldsymbol{L}^2(\partial\Omega)$, then $\boldsymbol{w} \in \boldsymbol{H}^{1+\frac{1}{2}}(\Omega)$ and

$$\|\boldsymbol{w}\|_{1+\frac{1}{2}} + \lambda\|div\boldsymbol{w}\|_{\frac{1}{2}} \leq C_R\|\boldsymbol{f}\|_{0,\partial\Omega}, \tag{2.7}$$

where the constant C_R is independent of μ and λ.

For any given $\boldsymbol{f} \in \boldsymbol{L}^2(\partial\Omega)$, from (2.7) we have $\boldsymbol{w} \in \boldsymbol{H}^{1+r}(\Omega), r < \frac{1}{2}$ and r can be arbitrarily close to $\frac{1}{2}$, and

$$\|\boldsymbol{w}\|_{1+r} + \lambda\|div\boldsymbol{w}\|_r \leq C_R\|\boldsymbol{f}\|_{0,\partial\Omega}. \tag{2.8}$$

Let $\boldsymbol{w}$ and $\boldsymbol{w}_h$ be the solution of (2.5) and (2.6), respectively, then the SIPG approximation (2.6) of (2.5) is consistent (see Lemma 3.3 in [6]):

$$a_h(\boldsymbol{w} - \boldsymbol{w}_h, \boldsymbol{v}_h) = 0, \ \forall \boldsymbol{v}_h \in \boldsymbol{S}^h. \tag{2.9}$$

For the source problem (2.5), let $\boldsymbol{f} \in \boldsymbol{L}^2(\partial\Omega)$, define the solution operator $A : \boldsymbol{L}^2(\partial\Omega) \to \boldsymbol{H}^1(\Omega)$ by

$$a(A\boldsymbol{f}, \boldsymbol{v}) = b(\boldsymbol{f}, \boldsymbol{v}), \ \forall \boldsymbol{v} \in \boldsymbol{H}^1(\Omega),$$

and define the operator $T : \boldsymbol{L}^2(\partial\Omega) \to \boldsymbol{L}^2(\partial\Omega)$:

$$T\boldsymbol{f} = (A\boldsymbol{f})',$$

where $'$ denotes the restriction on $\partial\Omega$. Then, (2.2) has the following equivalent operator form:

$$A\boldsymbol{u} = \frac{1}{\kappa}\boldsymbol{u}.$$

Similarly, from (2.6) we can define the discrete solution operator $A_h : \boldsymbol{L}^2(\partial\Omega) \to \boldsymbol{S}^h$ by

$$a_h(A_h\boldsymbol{f}, \boldsymbol{v}) = b_h(\boldsymbol{f}, \boldsymbol{v}), \ \forall \boldsymbol{v} \in \boldsymbol{S}^h,$$

and the operator $T_h : \boldsymbol{L}^2(\partial\Omega) \to \delta\boldsymbol{S}^h \subset \boldsymbol{L}^2(\partial\Omega)$ satisfying

$$T_h\boldsymbol{f} = (A_h\boldsymbol{f})',$$

where $\delta\boldsymbol{S}^h$ is the restriction of $\boldsymbol{S}^h$ on $\partial\Omega$. Then (2.3) has the following equivalent operator form:

$$A_h\boldsymbol{u}_h = \frac{1}{\kappa_h}\boldsymbol{u}_h.$$

Denote $\rho = \frac{1}{\kappa}, \rho_h = \frac{1}{\kappa_h}$. In this paper, κ, κ_h and ρ, ρ_h are all called eigenvalues.

From the definition of A_h and (2.4), noticing that $\|\cdot\|_h$ and $\|\cdot\|_G$ are equivalent on $\boldsymbol{S}^h$, we can deduce that

$$\|A_h\boldsymbol{f}\|_h^2 \lesssim a_h(A_h\boldsymbol{f}, A_h\boldsymbol{f}) = b_h(\boldsymbol{f}, A_h\boldsymbol{f}) \lesssim \|\boldsymbol{f}\|_{0,\partial\Omega}\|A_h\boldsymbol{f}\|_{0,\partial\Omega} \lesssim \|\boldsymbol{f}\|_{0,\partial\Omega}\|A_h\boldsymbol{f}\|_h,$$

thus,

$$\|A_h\boldsymbol{f}\|_h \leqslant C\|\boldsymbol{f}\|_{0,\partial\Omega} \leq C\|\boldsymbol{f}\|_h. \tag{2.10}$$

Reference [6] gave the a priori error estimates of DG approximation of (2.5).

Theorem 2.1. For any given $\boldsymbol{f} \in \boldsymbol{L}^2(\partial\Omega)$, let $\boldsymbol{w} \in \boldsymbol{H}^{1+r}(\Omega)(0 < r < \frac{1}{2})$ be the solution of (2.5), and let $\boldsymbol{w}_h$ be the solution of (2.6). Assume that the regularity estimate (2.8) is valid, then there hold

$$\|\boldsymbol{w} - \boldsymbol{w}_h\|_G \lesssim h^r \|\boldsymbol{f}\|_{0,\partial\Omega},$$
$$\|\boldsymbol{w} - \boldsymbol{w}_h\|_{0,\partial\Omega} \lesssim h^{2r} \|\boldsymbol{f}\|_{0,\partial\Omega};$$

Further, when $\boldsymbol{w} \in \boldsymbol{H}^{1+s}(\Omega)(\frac{1}{2} < s \leq k)$, there hold

$$\|\boldsymbol{w} - \boldsymbol{w}_h\|_h \lesssim h^r \left(\sqrt{2\mu}\|\boldsymbol{w}\|_{1+r} + \sqrt{\lambda}\|div\boldsymbol{w}\|_r \right),$$
$$\|\boldsymbol{w} - \boldsymbol{w}_h\|_{0,\partial\Omega} \lesssim h^{r+s} \left(\sqrt{2\mu}\|\boldsymbol{w}\|_{1+s} + \sqrt{\lambda}\|div\boldsymbol{w}\|_s \right).$$

Proof. See Theorems 3.6–3.8 in [6].

Suppose that κ is the jth eigenvalue of (2.2) with algebraic multiplicity q, i.e., $\kappa = \kappa_j = \kappa_{j+1} = \cdots = \kappa_{j+q-1}$. [5] proved that $\|T - T_h\|_{0,\partial\Omega} \to 0$ when $h \to 0$, therefore, q eigenvalues $\kappa_{j,h}, \kappa_{j+1,h}, \cdots, \kappa_{j+q-1,h}$ of (2.3) will converge to κ. Let $M(\kappa)$ be the space of eigenfunctions of (2.2) associated with eigenvalue κ, and $M_h(\kappa)$ be the direct sum of the generalized eigenspace of (2.3) associated with κ_h that converge to κ, $M(\rho) = M(\kappa)$ and $M_h(\rho) = M_h(\kappa)$. From [34] we have the following error estimates.

Theorem 2.2. Assume that the regularity estimate (2.8) is valid, and let $M(\kappa) \subset \boldsymbol{H}^{1+s}(\Omega)(\frac{1}{2} < s), t = \min\{k, s\}$, then there holds

$$|\kappa - \kappa_h| \lesssim h^{2t}; \tag{2.11}$$

Let $\boldsymbol{u}_h \in M_h(\kappa)$ be an eigenfunction of (2.3), then there exists $\boldsymbol{u} \in M(\kappa)$ such that

$$\|\boldsymbol{u} - \boldsymbol{u}_h\|_{0,\partial\Omega} \lesssim h^{r+t}, \tag{2.12}$$
$$\|\boldsymbol{u} - \boldsymbol{u}_h\|_h \lesssim h^t; \tag{2.13}$$

Let $\boldsymbol{u} \in M(\kappa)$ be an eigenfunction of (2.2), then there exists $\boldsymbol{u}_h \in M_h(\kappa)$ such that

$$\|\boldsymbol{u} - \boldsymbol{u}_h\|_h \lesssim h^t. \tag{2.14}$$

Proof. See Theorem 3.10 in [6] for the proofs of (2.11)–(2.13). By similar arguments we can get (2.14). □

3. Multigrid discretization

Let $\{\mathcal{T}_{h_i}\}_0^l$ be a family of regular meshes of Ω, $h_{i-1} \gg h_i$, and let $\boldsymbol{S}^{h_i}$ be the DG space defined on $\mathcal{T}_{h_i}$. Denote $\mathcal{T}_H = \mathcal{T}_{h_0}, \boldsymbol{S}^H = \boldsymbol{S}^{h_0}$. Now, for the eigenvalue problem (2.3) we give the following multigrid discretization scheme of DGFEM based on the shifted inverse iteration.

Scheme 3.1. Given the iteration times l.

Step 1: Solve (2.3) on $\boldsymbol{S}^H$: Find $(\kappa_H, \boldsymbol{u}_H) \in \mathbb{R} \times \boldsymbol{S}^H$, such that $\|\boldsymbol{u}_H\|_{0,\partial\Omega} = 1$ and

$$a_H(\boldsymbol{u}_H, \boldsymbol{v}) = \kappa_H b_H(\boldsymbol{u}_H, \boldsymbol{v}), \ \forall \boldsymbol{v} \in \boldsymbol{S}^H.$$

Step 2: $\boldsymbol{u}^{h_0} \Leftarrow \boldsymbol{u}_H, \kappa^{h_0} \Leftarrow \kappa_H, i \Leftarrow 1$.
Step 3: Solve a linear system on $\boldsymbol{S}^{h_i}$: Find $\boldsymbol{u}' \in \boldsymbol{S}^{h_i}$ such that

$$a_{h_i}(\boldsymbol{u}', \boldsymbol{v}) - \kappa^{h_{i-1}} b_{h_i}(\boldsymbol{u}', \boldsymbol{v}) = b_{h_i}(\boldsymbol{u}^{h_{i-1}}, \boldsymbol{v}), \ \forall \boldsymbol{v} \in \boldsymbol{S}^{h_i}.$$

Set $\boldsymbol{u}^{h_i} = \frac{\boldsymbol{u}'}{\|\boldsymbol{u}'\|_{0,\partial\Omega}}$.
Step 4: Compute the Rayleigh quotient

$$\kappa^{h_i} = \frac{a_{h_i}(\boldsymbol{u}^{h_i}, \boldsymbol{u}^{h_i})}{b_{h_i}(\boldsymbol{u}^{h_i}, \boldsymbol{u}^{h_i})}.$$

Step 5: If $i = l$, then output $(\kappa^{h_l}, \boldsymbol{u}^{h_l})$, stop; else, $i \Leftarrow i + 1$ and return to Step 3.

Next we will conduct the error analysis on Scheme 3.1.

From (2.9) we define the projection operator $P_h : \boldsymbol{H}^1(\Omega) + \boldsymbol{S}^h \to \boldsymbol{S}^h \subset \boldsymbol{L}^2(\partial\Omega)$ satifying

$$a_h(\boldsymbol{u} - P_h\boldsymbol{u}, \boldsymbol{v}_h) = 0, \qquad \forall \boldsymbol{v}_h \in \boldsymbol{S}^h. \tag{3.1}$$

Then, from (2.9) and (3.1) together with $A\boldsymbol{f} = \boldsymbol{w}, A_h\boldsymbol{f} = \boldsymbol{w}_h$, we can prove easily that $A_h = P_hA$.

We first give the following lemmas to prepare for the error analysis.

Lemma 3.1. Let $(\kappa, \boldsymbol{u})$ be an eigenpair of (2.2), then for any $\boldsymbol{v} \in \boldsymbol{S}^h$ and $\|\boldsymbol{v}\|_b \neq 0$, the Rayleigh quotient $R(\boldsymbol{v}) = \frac{a_h(\boldsymbol{v},\boldsymbol{v})}{\|\boldsymbol{v}\|_b^2}$ satisfies

$$R(\boldsymbol{v}) - \kappa = \frac{a_h(\boldsymbol{v} - \boldsymbol{u}, \boldsymbol{v} - \boldsymbol{u})}{\|\boldsymbol{v}\|_b^2} - \kappa\frac{\|\boldsymbol{v} - \boldsymbol{u}\|_b^2}{\|\boldsymbol{v}\|_b^2}. \tag{3.2}$$

Proof. From (2.9) we have

$$a_h(\boldsymbol{u}, \boldsymbol{v}) = b(\kappa\boldsymbol{u}, \boldsymbol{v}) = b_h(\kappa\boldsymbol{u}, \boldsymbol{v}), \quad \forall \boldsymbol{v} \in \boldsymbol{S}^h,$$

thus,

$$\begin{aligned}
& a_h(\boldsymbol{v} - \boldsymbol{u}, \boldsymbol{v} - \boldsymbol{u}) - \kappa b(\boldsymbol{v} - \boldsymbol{u}, \boldsymbol{v} - \boldsymbol{u}) \\
= \ & a_h(\boldsymbol{v}, \boldsymbol{v}) - 2a_h(\boldsymbol{u}, \boldsymbol{v}) + a_h(\boldsymbol{u}, \boldsymbol{u}) - \kappa b(\boldsymbol{v}, \boldsymbol{v}) + 2\kappa b(\boldsymbol{u}, \boldsymbol{v}) - \kappa b(\boldsymbol{u}, \boldsymbol{u}) \\
= \ & a_h(\boldsymbol{v}, \boldsymbol{v}) - 2b(\kappa\boldsymbol{u}, \boldsymbol{v}) + a(\boldsymbol{u}, \boldsymbol{u}) - \kappa b(\boldsymbol{v}, \boldsymbol{v}) + 2\kappa b(\boldsymbol{u}, \boldsymbol{v}) - \kappa b(\boldsymbol{u}, \boldsymbol{u}) \\
= \ & a_h(\boldsymbol{v}, \boldsymbol{v}) - \kappa b(\boldsymbol{v}, \boldsymbol{v}),
\end{aligned}$$

dividing both sides by $\|\boldsymbol{v}\|_b^2$ we obtain (3.2). □

Lemma 3.2. For any non-zero elements u, v in any normed linear space $(V, \|\cdot\|)$, it is valid that

$$\|\frac{u}{\|u\|} - \frac{v}{\|v\|}\| \leq 2\frac{\|u - v\|}{\|u\|}, \ \|\frac{u}{\|u\|} - \frac{v}{\|v\|}\| \leq 2\frac{\|u - v\|}{\|v\|}.$$

Proof. See Lemma 3.1 in [20]. □

Denote $d = dim\boldsymbol{S}^h$, $dist(\boldsymbol{u}, \boldsymbol{S}^h) = \inf\limits_{\boldsymbol{v}\in\boldsymbol{S}^h} \|\boldsymbol{u}-\boldsymbol{v}\|_h$. Referring to Lemma 4.1 in [20] we prove the following result which plays an important role in our analysis.

Lemma 3.3. Let $(\rho_0, \boldsymbol{w}_0)$ be an approximation of the jth eigenpair $(\rho, \boldsymbol{u})$ of (2.2) where ρ_0 is not an eigenvalue of A_h, $\boldsymbol{w}_0 \in \boldsymbol{S}^h$, $\|\boldsymbol{w}_0\|_{0,\partial\Omega} = 1$. And let $\boldsymbol{u}_0 = \frac{A_h\boldsymbol{w}_0}{\|A_h\boldsymbol{w}_0\|_{0,\partial\Omega}}$. Suppose that

$(C1)$ $\inf\limits_{\boldsymbol{v}\in M_h(\rho)} \|\boldsymbol{w}_0 - \boldsymbol{v}\|_{0,\partial\Omega} \le \frac{1}{2}$;

$(C2)$ $|\rho_0 - \rho| \le \frac{\vartheta}{4}, |\rho_{m,h} - \rho_m| \le \frac{\vartheta}{4}, m = j-1, j, j+q(m \ne 0)$, where $\vartheta = \min\limits_{m\ne j} |\rho_m - \rho|$ is the separate constant of the eigenvalue ρ;

$(C3)$ $\boldsymbol{u}' \in \boldsymbol{S}^h$ and $\boldsymbol{u}^h \in \boldsymbol{S}^h$ satisfy

$$(\rho_0 - A_h)\boldsymbol{u}' = \boldsymbol{u}_0, \quad \boldsymbol{u}^h = \frac{\boldsymbol{u}'}{\|\boldsymbol{u}'\|_{0,\partial\Omega}}. \tag{3.3}$$

Then

$$dist(\boldsymbol{u}^h, M_h(\rho)) \le \frac{C}{\vartheta} \max_{j\le m\le j+q-1} |\rho_0 - \rho_{m,h}| dist(\boldsymbol{w}_0, M_h(\rho)).$$

Proof. Let $\{\boldsymbol{u}_{m,h}\}_{m=1}^d$ be eigenfunctions of A_h satisfying $b(\boldsymbol{u}_{m,h}, \boldsymbol{u}_{i,h}) = \delta_{m,i}$. Then

$$\boldsymbol{u}_0 = \sum_{m=1}^{d} b(\boldsymbol{u}_0, \boldsymbol{u}_{m,h})\boldsymbol{u}_{m,h}.$$

Since ρ_0 is not an eigenvalue of A_h, from (3.3) we can get

$$\left(\rho_0 - \rho_{j,h}\right)\boldsymbol{u}' = \left(\rho_0 - \rho_{j,h}\right)(\rho_0 - A_h)^{-1}\boldsymbol{u}_0 = \sum_{m=1}^{d} \frac{\rho_0 - \rho_{j,h}}{\rho_0 - \rho_{m,h}} b(\boldsymbol{u}_0, \boldsymbol{u}_{m,h})\boldsymbol{u}_{m,h}. \tag{3.4}$$

Using triangle inequality and the condition $(C2)$ we derive

$$\begin{aligned} \left|\rho_0 - \rho_{j,h}\right| &\le |\rho_0 - \rho| + \left|\rho - \rho_{j,h}\right| \le \frac{\vartheta}{4} + \frac{\vartheta}{4} = \frac{\vartheta}{2}, \\ \left|\rho_0 - \rho_{m,h}\right| &\ge |\rho - \rho_m| - |\rho_0 - \rho| - \left|\rho_m - \rho_{m,h}\right| \ge \vartheta - \frac{\vartheta}{4} - \frac{\vartheta}{4} = \frac{\vartheta}{2}, \end{aligned}$$

where $m = j-1, j+q(m \ne 0)$. Hence, we have

$$\left|\rho_0 - \rho_{m,h}\right| \ge \frac{\vartheta}{2} \quad m \ne j, j+1, \cdots, j+q-1. \tag{3.5}$$

Because the operator T_h is selfadjoint with respect to $b(\cdot,\cdot)$, in fact, for $\forall \boldsymbol{f} \in \boldsymbol{L}^2(\partial\Omega)$, from the symmetry of $a_h(\cdot,\cdot)$ and $b(\cdot,\cdot)$ and $b(\cdot,\cdot) = b_h(\cdot,\cdot)$ we have $b(T_h\boldsymbol{f}, \boldsymbol{v_h}) = b(\boldsymbol{v_h}, T_h\boldsymbol{f}) = b_h(\boldsymbol{v_h}, T_h\boldsymbol{f}) = a_h(T_h\boldsymbol{v_h}, T_h\boldsymbol{f}) = a_h(T_h\boldsymbol{f}, T_h\boldsymbol{v_h}) = b_h(\boldsymbol{f}, T_h\boldsymbol{v_h}) = b(\boldsymbol{f}, T_h\boldsymbol{v_h})$ and $A_h\boldsymbol{u}_h = \rho_h\boldsymbol{u}_h$, then, for $m = 1, 2, \cdots, d$, there holds

$$\begin{aligned} b(T_h\boldsymbol{w}_0, \boldsymbol{u}_{m,h})\boldsymbol{u}_{m,h} &= b(\boldsymbol{w}_0, T_h\boldsymbol{u}_{m,h})\boldsymbol{u}_{m,h} = b(\boldsymbol{w}_0, \rho_{m,h}\boldsymbol{u}_{m,h})\boldsymbol{u}_{m,h} \\ &= b(\boldsymbol{w}_0, \boldsymbol{u}_{m,h})\rho_{m,h}\boldsymbol{u}_{m,h} = b(\boldsymbol{w}_0, \boldsymbol{u}_{m,h})A_h\boldsymbol{u}_{m,h}. \end{aligned} \tag{3.6}$$

Noticing that $\{\boldsymbol{u}_{m,h}\}_{m=j}^{j+q-1}$ is a standard orthogonal basis of $M_h(\rho)$ with respect to the $\boldsymbol{L}^2(\partial\Omega)$ inner product $b(\cdot,\cdot)$, from $\boldsymbol{u}_0 = \frac{A_h\boldsymbol{w}_0}{\|A_h\boldsymbol{w}_0\|_{0,\partial\Omega}}$, (3.4), (3.6), (2.10) and (3.5) we deduce

$$
\begin{aligned}
&\|(\rho_0-\rho_{j,h})\boldsymbol{u}' - \sum_{m=j}^{j+q-1}\frac{\rho_0-\rho_{j,h}}{\rho_0-\rho_{m,h}}b(\boldsymbol{u}_0,\boldsymbol{u}_{m,h})\boldsymbol{u}_{m,h}\|_h\\
=\;& \|\sum_{m\neq j,j+1,\cdots,j+q-1}\frac{\rho_0-\rho_{j,h}}{\rho_0-\rho_{m,h}}b(\boldsymbol{u}_0,\boldsymbol{u}_{m,h})\boldsymbol{u}_{m,h}\|_h\\
=\;& \frac{1}{\|A_h\boldsymbol{w}_0\|_{0,\partial\Omega}}\left\|\sum_{m\neq j,j+1,\cdots,j+q-1}\frac{\rho_0-\rho_{j,h}}{\rho_0-\rho_{m,h}}b(A_h\boldsymbol{w}_0,\boldsymbol{u}_{m,h})\boldsymbol{u}_{m,h}\right\|_h\\
=\;& \frac{1}{\|A_h\boldsymbol{w}_0\|_{0,\partial\Omega}}\left\|\sum_{m\neq j,j+1,\cdots,j+q-1}\frac{\rho_0-\rho_{j,h}}{\rho_0-\rho_{m,h}}b(T_h\boldsymbol{w}_0,\boldsymbol{u}_{m,h})\boldsymbol{u}_{m,h}\right\|_h\\
=\;& \frac{1}{\|A_h\boldsymbol{w}_0\|_{0,\partial\Omega}}\left\|\sum_{m\neq j,j+1,\cdots,j+q-1}\frac{\rho_0-\rho_{j,h}}{\rho_0-\rho_{m,h}}b(\boldsymbol{w}_0,\boldsymbol{u}_{m,h})A_h\boldsymbol{u}_{m,h}\right\|_h\\
=\;& \frac{1}{\|A_h\boldsymbol{w}_0\|_{0,\partial\Omega}}\left\|A_h\left(\sum_{m\neq j,j+1,\cdots,j+q-1}\frac{\rho_0-\rho_{j,h}}{\rho_0-\rho_{m,h}}b(\boldsymbol{w}_0,\boldsymbol{u}_{m,h})\boldsymbol{u}_{m,h}\right)\right\|_h\\
\le\;& \frac{C}{\|A_h\boldsymbol{w}_0\|_{0,\partial\Omega}}\left\|\sum_{m\neq j,j+1,\cdots,j+q-1}\frac{\rho_0-\rho_{j,h}}{\rho_0-\rho_{m,h}}b(\boldsymbol{w}_0,\boldsymbol{u}_{m,h})\boldsymbol{u}_{m,h}\right\|_{0,\partial\Omega}\\
\le\;& \frac{2C}{\vartheta\|A_h\boldsymbol{w}_0\|_{0,\partial\Omega}}\left|\rho_0-\rho_{j,h}\right|\left(\sum_{m\neq j,j+1,\cdots,j+q-1}b^2(\boldsymbol{w}_0,\boldsymbol{u}_{m,h})\right)^{\frac{1}{2}}\\
\le\;& \frac{2C}{\vartheta\|A_h\boldsymbol{w}_0\|_{0,\partial\Omega}}\left|\rho_0-\rho_{j,h}\right|\left\|\boldsymbol{w}_0-\sum_{m=j}^{j+q-1}b(\boldsymbol{w}_0,\boldsymbol{u}_{m,h})\boldsymbol{u}_{m,h}\right\|_{0,\partial\Omega}\\
=\;& \frac{2C}{\vartheta\|A_h\boldsymbol{w}_0\|_{0,\partial\Omega}}\left|\rho_0-\rho_{j,h}\right|\inf_{\boldsymbol{v}\in M_h(\rho)}\|\boldsymbol{w}_0-\boldsymbol{v}\|_{0,\partial\Omega}\\
\le\;& \frac{2C}{\vartheta\|A_h\boldsymbol{w}_0\|_{0,\partial\Omega}}\left|\rho_0-\rho_{j,h}\right|\operatorname{dist}(\boldsymbol{w}_0,M_h(\rho)).
\end{aligned}
\tag{3.7}
$$

Taking the norm on both sides of (3.4), and noting that $\boldsymbol{u}_0 = \frac{A_h\boldsymbol{w}_0}{\|A_h\boldsymbol{w}_0\|_{0,\partial\Omega}}$, the condition $(C1)$ and (3.6), we get

$$
\begin{aligned}
\left\|\left(\rho_0-\rho_{j,h}\right)\boldsymbol{u}'\right\|_{0,\partial\Omega} &= \frac{1}{\|A_h\boldsymbol{w}_0\|_{0,\partial\Omega}}\left\|\sum_{m=1}^{d}\frac{\rho_0-\rho_{j,h}}{\rho_0-\rho_{m,h}}b(A_h\boldsymbol{w}_0,\boldsymbol{u}_{m,h})\boldsymbol{u}_{m,h}\right\|_{0,\partial\Omega}\\
&= \frac{1}{\|A_h\boldsymbol{w}_0\|_{0,\partial\Omega}}\left\|\sum_{m=1}^{d}\frac{\rho_0-\rho_{j,h}}{\rho_0-\rho_{m,h}}b(T_h\boldsymbol{w}_0,\boldsymbol{u}_{m,h})\boldsymbol{u}_{m,h}\right\|_{0,\partial\Omega}\\
&= \frac{1}{\|A_h\boldsymbol{w}_0\|_{0,\partial\Omega}}\left(\sum_{m=1}^{d}\left(\frac{\rho_0-\rho_{j,h}}{\rho_0-\rho_{m,h}}b^2(\boldsymbol{w}_0,\rho_{m,h}\boldsymbol{u}_{m,h})\right)\right)^{\frac{1}{2}}
\end{aligned}
$$

$$\geq \frac{C}{\|A_h \boldsymbol{w}_0\|_{0,\partial\Omega}} \min_{j\leq m\leq j+q-1} \left|\frac{\rho_0-\rho_{j,h}}{\rho_0-\rho_{m,h}}\right| \left(\sum_{m=j}^{j+q-1} b^2(\boldsymbol{w}_0, \boldsymbol{u}_{m,h})\right)^{\frac{1}{2}}$$

$$= \frac{C}{\|A_h \boldsymbol{w}_0\|_{0,\partial\Omega}} \min_{j\leq m\leq j+q-1} \left|\frac{\rho_0-\rho_{j,h}}{\rho_0-\rho_{m,h}}\right| \left\|\boldsymbol{w}_0 - \left(\boldsymbol{w}_0 - \sum_{m=j}^{j+q-1} b(\boldsymbol{w}_0, \boldsymbol{u}_{m,h})\boldsymbol{u}_{m,h}\right)\right\|_{0,\partial\Omega}$$

$$\geq \frac{C}{2\,\|A_h \boldsymbol{w}_0\|_{0,\partial\Omega}} \min_{j\leq m\leq j+q-1} \left|\frac{\rho_0-\rho_{j,h}}{\rho_0-\rho_{m,h}}\right|. \tag{3.8}$$

From (3.7) and (3.8) we derive

$$\begin{aligned}
&\operatorname{dist}\left(\boldsymbol{u}^h, M_h(\rho)\right) = \operatorname{dist}\left(\operatorname{sign}\left(\rho_0-\rho_{j,h}\right)\boldsymbol{u}^h, M_h(\rho)\right)\\
\leq\ & \left\|\operatorname{sign}\left(\rho_0-\rho_{j,h}\right)\boldsymbol{u}^h - \frac{1}{\left\|\left(\rho_0-\rho_{j,h}\right)\boldsymbol{u}'\right\|_{0,\partial\Omega}} \sum_{m=j}^{j+q-1} \frac{\rho_0-\rho_{j,h}}{\rho_0-\rho_{m,h}} b(\boldsymbol{u}_0, \boldsymbol{u}_{m,h})\boldsymbol{u}_{m,h}\right\|_h\\
=\ & \left\|\frac{\left(\rho_0-\rho_{j,h}\right)\boldsymbol{u}'}{\left\|\left(\rho_0-\rho_{j,h}\right)\boldsymbol{u}'\right\|_{0,\partial\Omega}} - \frac{1}{\left\|\left(\rho_0-\rho_{j,h}\right)\boldsymbol{u}'\right\|_{0,\partial\Omega}} \sum_{m=j}^{j+q-1} \frac{\rho_0-\rho_{j,h}}{\rho_0-\rho_{m,h}} b(\boldsymbol{u}_0, \boldsymbol{u}_{m,h})\boldsymbol{u}_{m,h}\right\|_h\\
\leq\ & \frac{2}{C}\|A_h \boldsymbol{w}_0\|_{0,\partial\Omega} \max_{j\leq m\leq j+q-1} \left|\frac{\rho_0-\rho_{m,h}}{\rho_0-\rho_{j,h}}\right| \left\|\left(\rho_0-\rho_{j,h}\right)\boldsymbol{u}' - \sum_{m=j}^{j+q-1} \frac{\rho_0-\rho_{j,h}}{\rho_0-\rho_{m,h}} b(\boldsymbol{u}_0, \boldsymbol{u}_{m,h})\boldsymbol{u}_{m,h}\right\|_h\\
\leq\ & \frac{C}{\vartheta} \max_{j\leq m\leq j+q-1} \left|\rho_0-\rho_{m,h}\right| \operatorname{dist}\left(\boldsymbol{w}_0, M_h(\rho)\right).
\end{aligned}$$

The proof is completed. □

Now we can analyze the error of multigrid discretization scheme 3.1 by using Theorem 2.2 and Lemma 3.3. We first consider the case of $l = 1$. Denote $H = h_0, h = h_1$.

Theorem 3.1. Suppose that $M(\kappa_j) \subset \boldsymbol{H}^{1+s}(\Omega)(s \geq r)$, and $t = \min\{k, s\}$. Let $(\kappa_j^h, \boldsymbol{u}_j^h)$ be an approximate eigenpair obtained by Scheme 3.1 ($l = 1$) and H is sufficiently small, then there exists $\boldsymbol{u}_j \in M(\kappa_j)$ such that

$$\left\|\boldsymbol{u}_j^h - \boldsymbol{u}_j\right\|_h \leq C(H^{3t} + h^t), \tag{3.9}$$

$$\left\|\boldsymbol{u}_j^h - \boldsymbol{u}_j\right\|_{0,\partial\Omega} \leq C(H^{3t} + h^{r+t}), \tag{3.10}$$

$$|\kappa_j^h - \kappa_j| \leq C\left(H^{3t} + h^t\right)^2. \tag{3.11}$$

Proof. We will use Lemma 3.3 to complete the proof. Take $\rho_0 = \frac{1}{\kappa_H}, \boldsymbol{w}_0 = \boldsymbol{u}_H$ and $\boldsymbol{u}_0 = \frac{A_h \boldsymbol{u}_H}{\|A_h \boldsymbol{u}_H\|_{0,\partial\Omega}}$. From (2.13) we know that there exists $\bar{\boldsymbol{u}} \in M(\kappa_j)$ such that

$$\|\boldsymbol{u}_H - \bar{\boldsymbol{u}}\|_h \leq CH^t.$$

From the triangle inequality and (2.14) we have

$$\begin{aligned}
dist(\boldsymbol{u}_H, M_h(\kappa_j)) &\leq \|\boldsymbol{u}_H - \bar{\boldsymbol{u}}\|_H + dist(\bar{\boldsymbol{u}}, M_h(\kappa_j))\\
&\leq C(H^t + h^t) \leq CH^t,
\end{aligned} \tag{3.12}$$

thus,

$$\inf_{\boldsymbol{v}\in M_h(\kappa_j)} \|\boldsymbol{u}_H - \boldsymbol{v}\|_{0,\partial\Omega} \le CH^t,$$

when H is small enough, the condition $(C1)$ in Lemma 3.3 is valid.

From (2.11) we get

$$\begin{aligned} \left|\rho_0 - \rho_j\right| &= \frac{\left|\kappa_H - \kappa_j\right|}{|\kappa_H\kappa_j|} \le CH^{2t} \le \frac{\vartheta}{4}; \\ \left|\rho_m - \rho_{m,h}\right| &= \frac{\left|\kappa_{m,h} - \kappa_m\right|}{|\kappa_{m,h}\kappa_m|} \le Ch^{2t} \le \frac{\vartheta}{4}, \quad m = j-1, j, \ldots, j+q, m \ne 0, \end{aligned}$$

i.e., the condition $(C2)$ in Lemma 3.3 holds.

From the definition of A_h we know that Step 3 in Scheme 3.1 is equivalent to the following:

$$a_h(\boldsymbol{u}', \boldsymbol{v}) - \kappa_H a_h(A_h\boldsymbol{u}', \boldsymbol{v}) = a_h(A_h\boldsymbol{u}_H, \boldsymbol{v}) \quad \forall \boldsymbol{v} \in \boldsymbol{S}^h,$$

and $\boldsymbol{u}_j^h = \frac{\boldsymbol{u}'}{\|\boldsymbol{u}'\|_{0,\partial\Omega}}$, i.e.,

$$\left(\kappa_H^{-1} - A_h\right)\boldsymbol{u}' = \kappa_H^{-1}A_h\boldsymbol{u}_H, \quad \boldsymbol{u}_j^h = \frac{\boldsymbol{u}'}{\|\boldsymbol{u}'\|_{0,\partial\Omega}}.$$

Note that $\kappa_H^{-1}A_h\boldsymbol{u}_H$ and $\boldsymbol{u}_0$ differ by only one constant, thus, Step 3 in Scheme 3.1 is equivalent to

$$\left(\kappa_H^{-1} - A_h\right)\boldsymbol{u}' = \boldsymbol{u}_0, \quad \boldsymbol{u}_j^h = \frac{\boldsymbol{u}'}{\|\boldsymbol{u}'\|_{0,\partial\Omega}}.$$

So far, all conditions of Lemma 3.3 are valid.

Since $M_h(\kappa_j)$ is a q-dimensional space, there must exist $\boldsymbol{u}^* \in M_h(\kappa_j)$ such that

$$\left\|\boldsymbol{u}_j^h - \boldsymbol{u}^*\right\|_h = \operatorname{dist}\left(\boldsymbol{u}_j^h, M_h(\kappa_j)\right).$$

For $m = j, j+1, \ldots, j+q-1$, according to (2.11) we have

$$\begin{aligned} |\,\rho_0 - \rho_{m,h}\,| &= |\frac{1}{\kappa_H} - \frac{1}{\kappa_{m,h}}| \le \frac{\left|\kappa_H - \kappa_{m,h}\right|}{\left|\kappa_H\kappa_{m,h}\right|} \\ &\le C(|\kappa_H - \kappa_j| + |\kappa_j - \kappa_{m,h}|) \le CH^{2t}. \end{aligned} \tag{3.13}$$

Therefore, from Lemma 3.3, (3.12) and (3.13) we get

$$\begin{aligned} &\|\boldsymbol{u}_j^h - \boldsymbol{u}^*\|_h = \operatorname{dist}\left(\boldsymbol{u}_j^h, M_h(\kappa_j)\right) \\ \le\ & \frac{C}{\vartheta}\max_{j\le m\le j+q-1}\left|\rho_0 - \rho_{m,h}\right|\operatorname{dist}\left(\boldsymbol{u}_H, M_h(\kappa_j)\right) \le CH^{3t}. \end{aligned} \tag{3.14}$$

From (2.13) we know that there exists $\boldsymbol{u}_j \in M(\kappa_j)$, such that $\|\boldsymbol{u}^* - \boldsymbol{u}_j\|_h = \operatorname{dist}\left(\boldsymbol{u}^*, M(\kappa_j)\right)$, and

$$\|\boldsymbol{u}^* - \boldsymbol{u}_j\|_h \le Ch^t,$$

then

$$\|\boldsymbol{u}_j^h - \boldsymbol{u}_j\|_h \le \|\boldsymbol{u}_j^h - \boldsymbol{u}^*\|_h + \|\boldsymbol{u}^* - \boldsymbol{u}_j\|_h \le C(H^{3t} + h^t),$$

that is (3.9).

Next, we will prove (3.10). From (2.12) we have

$$\|\boldsymbol{u}^* - \boldsymbol{u}_j\|_{0,\partial\Omega} \le Ch^{r+t},$$

which together with (3.14) yields

$$\|\boldsymbol{u}_j^h - \boldsymbol{u}_j\|_{0,\partial\Omega} \le \|\boldsymbol{u}_j^h - \boldsymbol{u}^*\|_{0,\partial\Omega} + \|\boldsymbol{u}^* - \boldsymbol{u}_j\|_{0,\partial\Omega} \le C(H^{3t} + h^{r+t}).$$

Finally, we use Lemma 3.1 to derive (3.11). From Step 4 of Scheme 3.1, Lemma 3.1, (3.9) and (3.10) we deduce that

$$\begin{aligned} |\kappa_j^h - \kappa_j| &= \left| \frac{a_h(\boldsymbol{u}_j^h - \boldsymbol{u}_j, \boldsymbol{u}_j^h - \boldsymbol{u}_j)}{\|\boldsymbol{u}_j^h\|_b^2} - \kappa_j \frac{b(\boldsymbol{u}_j^h - \boldsymbol{u}_j, \boldsymbol{u}_j^h - \boldsymbol{u}_j)}{\|\boldsymbol{u}_j^h\|_b^2} \right| \\ &\le C\left(\|\boldsymbol{u}_j^h - \boldsymbol{u}_j\|_h^2 + |\kappa_j| \|\boldsymbol{u}_j^h - \boldsymbol{u}_j\|_{0,\partial\Omega}^2 \right) \\ &\le C\left(H^{3t} + h^t \right)^2. \end{aligned}$$

The proof is completed. □

Remark 3.1. Using Theorem 3.1 and referring to Theorem 4.2 in [32], we can give the error estimates of Scheme 3.1. To ensure that the error is independent of the number of iterations in the multigrid refinement, we also need the following conditions.

Condition 3.1. For any given $\varepsilon \in (0, 1)$, there exists $t_i \in (1, 2 - \varepsilon](i = 1, 2, \cdots)$, such that $h_i = O(h_{i-1}^{t_i})$, and $h_i \to 0$ $(i \to \infty)$.

Condition 3.1 is easy to be satisfied. For instance, for smooth eigenfunctions, using uniform meshes and linear elements and taking $\varepsilon = 0.1, h_0 = \frac{\sqrt{2}}{8}, h_1 = \frac{\sqrt{2}}{32}, h_2 = \frac{\sqrt{2}}{128}, \cdots$, then $t_i = \frac{log(h_i)}{log(h_{i-1})} = \frac{log(h_{i-1}) - log(4)}{log(h_{i-1})}$, thus, $t_1 \approx 1.80, t_2 \approx 1.44, t_3 \approx 1.31, \cdots$, and $t_i \searrow 1$ when $i \to \infty$.

Theorem 3.2. Suppose that Condition 3.1 holds and $M(\kappa_j) \subset H^{1+s}(\Omega)$ $(s \ge r)$, and $t = \min\{k, s\}$. Let $(\kappa_j^{h_l}, \boldsymbol{u}_j^{h_l})$ be an approximate eigenpair obtained by Scheme 3.1, then, when $h_0 = H$ is small enough, there exists $\boldsymbol{u}_j \in M(\kappa_j)$ such that

$$\left\| \boldsymbol{u}_j^{h_l} - \boldsymbol{u}_j \right\|_h \le Ch_l^t, \tag{3.15}$$

$$\left\| \boldsymbol{u}_j^{h_l} - \boldsymbol{u}_j \right\|_{0,\partial\Omega} \le Ch_l^{r+t}, \tag{3.16}$$

$$\left| \kappa_j^{h_l} - \kappa_j \right| \le Ch_l^{2t}, \quad l \ge 1. \tag{3.17}$$

4. Numerical experiments

In this section, we will report some numerical experiments to show the efficiency of the DG-multigrid method (Scheme 3.1) for solving the Steklov-Lamé eigenproblem. We conduct the

numerical experiments on the MATLAB 2022a on a ThinkBook 14p Gen 2 PC with 16G memory, and our program makes use of the package of iFEM [35]. The test domains are set to be the unit square $\Omega_S = (0,1)^2$ and the L-shaped domain $\Omega_L = (-1,1)^2\backslash[0,1)^2$.

Example 4.1. We use Scheme 3.1 to compute the approximation for the 1st eigenvalue κ_1 of the problem (2.2). We adopt piecewise polynomial of degree 1 ($P1$ element) to compute on uniform isosceles right triangulations. We produce the initial coarse grid $\mathcal{T}_H = \mathcal{T}_{h_0}$ and refine the coarse grid in a uniform way (each triangle is divided into four congruent triangles) repeatedly to obtain fine grids $\mathcal{T}_{h_i}, i = 1, 2, ..., l$. By using the basis functions of $\boldsymbol{S}^H$, the eigenvalue problem on the initial coarse grid in Step 1 of Scheme 3.1 can be rewritten as a generalized matrix eigenvalue problem

$$K^H \bar{\boldsymbol{u}}_{1,H} = \kappa_{1,H} M^H \bar{\boldsymbol{u}}_{1,H}, \tag{4.1}$$

where the elements of array $\bar{\boldsymbol{u}}_{1,H}$ are the coordinates of $\boldsymbol{u}_{1,H}$ under the basis functions in $\boldsymbol{S}^H$. Similarly, by using the basis functions of $\boldsymbol{S}^{h_i}$, the algebraic system in Step 3 of Scheme 3.1 can be rewritten as

$$(K^{h_i} - \kappa_1^{h_{i-1}} M^{h_i})\hat{\boldsymbol{u}} = M^{h_i} \hat{\boldsymbol{u}}_1^{h_{i-1}} \tag{4.2}$$

and $\bar{\boldsymbol{u}}_1^{h_i} = \frac{\hat{\boldsymbol{u}}}{\sqrt{\hat{\boldsymbol{u}}^T M^{h_i} \hat{\boldsymbol{u}}}}$ where $\hat{\boldsymbol{u}}_1^{h_{i-1}}$ is actually the projection of the solution $\bar{\boldsymbol{u}}_1^{h_{i-1}}$ obtained on the previous grid $\mathcal{T}_{h_{i-1}}$ in $\mathcal{T}_{h_i}$. For example, if $\mathcal{T}_{h_0}$ contains $NT = 2$ elements with the associated solution $\bar{\boldsymbol{u}}_1^{h_0} = \bar{\boldsymbol{u}}_{1,H}$, denote $\bar{\boldsymbol{u}}_1^{h_0} = [u_1^{h_0}, u_2^{h_0}]^T$ with $u_1^{h_0} = [a_{11}, a_{21}, a_{12}, a_{22}, a_{13}, a_{23}]$, $u_2^{h_0} = [b_{11}, b_{21}, b_{12}, b_{22}, b_{13}, b_{23}]$ and $a_{\iota j}, b_{\iota j} (j = 1, 2, 3)$ being the coordinates of the basis function $\{1, x, y\}$ on the element ι in $\mathcal{T}_{h_0}$, and encrypt $\mathcal{T}_{h_0}$ once (each triangle is divided into four congruent triangles) to get $\mathcal{T}_{h_1}$ which contains $4NT = 8$ elements, then the projection of $\bar{\boldsymbol{u}}_1^{h_0}$ in $\mathcal{T}_{h_1}$ is as follows:

$$\hat{\boldsymbol{u}}_1^{h_0} = Q_1 \bar{\boldsymbol{u}}_1^{h_0},$$

where Q_1 is the projection (restriction) operator:

$$Q_1 = \begin{bmatrix} Q_{11} & 0 \\ 0 & Q_{12} \end{bmatrix},\ Q_{11} = Q_{12} = \begin{bmatrix} I_{NT}^4 & 0 & 0 \\ 0 & I_{NT}^4 & 0 \\ 0 & 0 & I_{NT}^4 \end{bmatrix},\ I_{NT}^4 = \begin{bmatrix} I_{NT} \\ I_{NT} \\ I_{NT} \\ I_{NT} \end{bmatrix},\ I_{NT} = I_2 = \begin{bmatrix} 1 & 0 \\ 0 & 1 \end{bmatrix}.$$

If bisecting encryption is used, that is, each triangle is divided into two triangles, then just replace I_{NT}^4 with $I_{NT}^2 = \begin{bmatrix} I_{NT} \\ I_{NT} \end{bmatrix}$. We use the command "eigs" of MATLAB to solve the discrete algebraic eigenvalue problem (4.1), and use the command "\" in MATLAB to solve the linear system (4.2). Further, there has no difficulty with solving the system (4.2) (see Lecture 27.4 in [36]).

For comparison, we also use the multigrid method of conforming finite elements by adopting $P1$ element to compute. The error curves are depicted in Figure 1 where the reference value are taken as the most accurate approximations that we can compute. From Figure 1, we can see that as the Lamé parameter λ increases, the DG-multigrid method is robust compared with the multigrid method of conforming finite elements, which is a major advantage of using DG method to solve elastic problems.

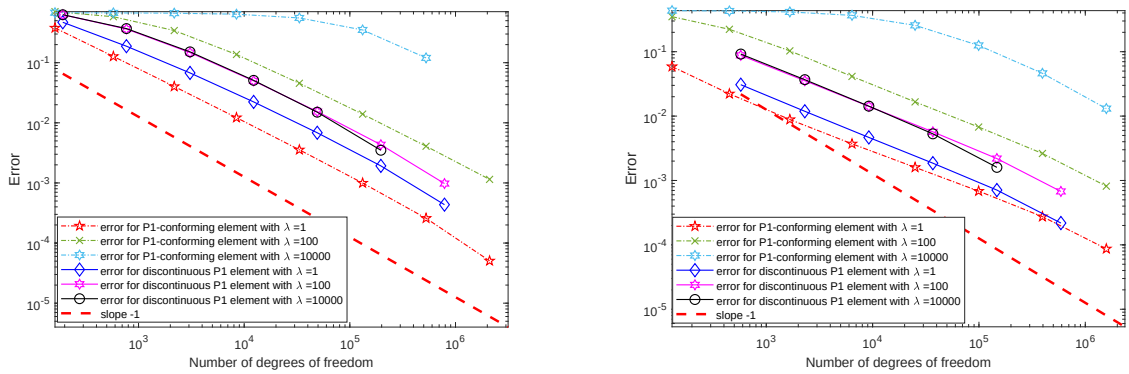

Figure 1. The error curves of the approximations for the 1st eigenvalue κ_1 of (2.2) obtained by multigrid method of conforming finite element and the DG-multigrid method by using $P1$ element in Ω_S (left) and Ω_L (right).

Example 4.2. Adaptive computation.

Adaptive algorithm based on the a posterior error estimation is an efficient and important numerical approach for solving partial differential equations. Referring to [37], we combine the multigrid scheme 3.1 and the a posteriori error indicator to establish the adaptive multigrid algorithm. Referring to the a posterior error indicator (25) for the linear elastic source problem in [37], we formally give the following local error indicator for the underlying eigenvalue problem:

$$\begin{aligned}\zeta_K^2(\kappa_h, \boldsymbol{u}_h) &= h_K^2 \|div\boldsymbol{\sigma}(\boldsymbol{u}_h)\|_{L^2(K)}^2 + h_K \Big(\|\Sigma_{\boldsymbol{n}}(\boldsymbol{u}_h) - \boldsymbol{n}\cdot\boldsymbol{\sigma}(\boldsymbol{u}_h)\|_{L^2(\partial K\setminus\partial\Omega)}^2 \\ &\quad + \|\Sigma_{\boldsymbol{n}}(\boldsymbol{u}_h) - \boldsymbol{n}\cdot\boldsymbol{\sigma}(\boldsymbol{u}_h)\|_{L^2(\partial K\cap\partial\Omega)}^2 \Big) + h_K^{-1} \|[\![\boldsymbol{u}_h]\!]\|_{L^2(\partial K\setminus\partial\Omega)}^2,\end{aligned}$$

where

$$\Sigma_{\boldsymbol{n}}(\boldsymbol{u}_h) := \begin{cases} \boldsymbol{n}\cdot\{\boldsymbol{\sigma}(\boldsymbol{u}_h)\} - \gamma_\mu h_e^{-1}[\![\boldsymbol{u}_h]\!] - h_e^{-1}\gamma_\lambda \boldsymbol{n}(\boldsymbol{n}\cdot[\![\boldsymbol{u}_h]\!]), & on\ \partial K\setminus\partial\Omega, \\ (\kappa_h - 1)\boldsymbol{u}_h, & on\ \partial K\cap\partial\Omega. \end{cases}$$

Define the global error indicator:

$$\zeta_\Omega = \Big(\sum_{K\in\mathcal{T}_h} \zeta_K^2(\kappa_h, \boldsymbol{u}_h)\Big)^{\frac{1}{2}}.$$

Based on the above error indicators and Scheme 3.1, we design the following adaptive multigrid algorithm bases on the shifted inverse iteration.

Algorithm 4.1. Choose parameter $0 < \alpha < 1$.

Step 1: Pick any initial mesh $\mathcal{T}_{h_0}$.

Step 2: Solve (2.3) on $\mathcal{T}_{h_0}$ for discrete solution $(\kappa_{j,h_0}, \boldsymbol{u}_{j,h_0})$.

Step 3: Let $l = 1$. $\boldsymbol{u}_j^{h_1} \Leftarrow \boldsymbol{u}_{j,h_0}, \kappa_j^{h_1} \Leftarrow \kappa_{j,h_0}$.

Step 4: Compute the local indicator $\zeta_K(\kappa_j^{h_l}, \boldsymbol{u}_j^{h_l})$.

Step 5: Construct $\widehat{\mathcal{T}}_{h_l} \subset \mathcal{T}_{h_l}$ by Mark Strategy and parameter α.

Step 6: Refine $\mathcal{T}_{h_l}$ to get a new mesh $\mathcal{T}_{h_{l+1}}$ by procedure REFINE.

Step 7: Find $\widetilde{\boldsymbol{u}} \in \boldsymbol{S}^{h_{l+1}}$ such that

$$a_{h_{l+1}}(\widetilde{\boldsymbol{u}}, \boldsymbol{\psi}) - \kappa_j^{h_l} b_{h_{l+1}}(\widetilde{\boldsymbol{u}}, \boldsymbol{\psi}) = b_{h_{l+1}}(\boldsymbol{u}_j^{h_l}, \boldsymbol{\psi}),\ \forall \boldsymbol{\psi} \in \boldsymbol{S}^{h_{l+1}}.$$

Denote $\boldsymbol{u}_j^{h_{l+1}} = \frac{\widetilde{\boldsymbol{u}}}{|\widetilde{\boldsymbol{u}}|_{0,\partial\Omega}}$ and compute the Rayleigh quotient

$$\kappa_j^{h_{l+1}} = \frac{a_{h_{l+1}}(\boldsymbol{u}_j^{h_{l+1}}, \boldsymbol{u}_j^{h_{l+1}})}{b_{h_{l+1}}(\boldsymbol{u}_j^{h_{l+1}}, \boldsymbol{u}_j^{h_{l+1}})}.$$

Step 8: Let $l = l + 1$ and go to Step 4.

Mark Strategy

Given parameter $0 < \alpha < 1$.

Step 1: Construct a minimal subset $\widehat{\mathcal{T}}_{h_l}$ of $\mathcal{T}_{h_l}$ by selecting some elements in $\mathcal{T}_{h_l}$ such that

$$\sum_{K\in\widehat{\mathcal{T}}_{h_l}} \zeta_K^2(\kappa_j^{h_l}, \boldsymbol{u}_j^{h_l}) \geq \alpha \sum_{K\in\mathcal{T}_{h_l}} \zeta_K^2(\kappa_j^{h_l}, \boldsymbol{u}_j^{h_l}).$$

Step 2: Mark all elements in $\widehat{\mathcal{T}}_{h_l}$.

Mark Strategy was first proposed in [38], and the procedure REFINE is some iterative or recursive bisection (see, e.g., [39, 40]) of elements with the minimal refinement condition that marked elements are bisected at least once.

In addition, to investigate the efficiency of Algorithm 4.1, referring to the standard popular adaptive algorithm [41] we give the following Algorithm 4.2 for comparison.

Algorithm 4.2. Choose parameter $0 < \alpha < 1$.

Step 1: Pick any initial mesh $\mathcal{T}_{h_0}$.

Step 2: Solve (2.3) on $\mathcal{T}_{h_0}$ for discrete solution $(\kappa_{j,h_1}, \boldsymbol{u}_{j,h_1})$.

Step 3: Let $l = 1$.

Step 4: Compute the local indicators $\zeta_K(\kappa_{j,h_l}, \boldsymbol{u}_{j,h_l})$.

Step 5: Construct $\widehat{\mathcal{T}}_{h_l} \subset \mathcal{T}_{h_l}$ by Mark Strategy and parameter α.

Step 6: Refine $\mathcal{T}_{h_l}$ to get a new mesh $\mathcal{T}_{h_{l+1}}$ by procedure REFINE.

Step 7: Solve (2.3) on $\mathcal{T}_{h_{l+1}}$ for discrete solution $(\kappa_{j,h_{l+1}}, \boldsymbol{u}_{j,h_{l+1}})$.

Step 8: Let $l = l + 1$ and go to Step 4.

We use the adaptive DG-multigrid method (Algorithm 4.1) with polynomials of degree 1 ($P1$ element) and degree 2 ($P2$ element) to compute, and take $\alpha = 0.5$. For convenience of reading, we specify the following notations in our tables and figures.

- $N_{j,l}$: the degrees of freedom at the lth iteration;
- $\kappa_j^{h_l}$: the jth eigenvalue obtained by Algorithm 4.1 at the l th iteration;
- κ_{j,h_l}: the jth eigenvalue obtained by Algorithm 4.2 at the l th iteration;
- $CPU_{j,l}(s)$: the CPU time(s) from the first iteration beginning to the calculate results of the lth iteration appearing by using Algorithm 4.1/4.2;
- e_j: the error of the jth approximate eigenvalue by Algorithm 4.1;
- ζ_j: the error indicator of the jth approximate eigenvalue by Algorithm 4.1.

We first give a numerical experiment comparison between using DGFEM to solve directly on fine meshes and using the adaptive DG-multigrid method (Algorithm 4.1) for the 1st nonzero eigenvalue of (2.3). The error curves are shown in Figures 2 and 3. An observation of the left and right subgraphs in Figures 2 and 3 tells us that the regularity of the eigenfunction in Ω_L is lower than that in Ω_S, which

is consistent with the general conclusion of the regularity of solutions to PDEs. From Figure 2 we can see that the error curves of adaptive DG-multigrid method are all parallel to the line with slope -1 but the error curves of directly computing by DGFEM do not parallel, which indicates that the approximate eigenvalues obtained by the adaptive DG-multigrid method achieve the optimal convergence order. The same conclusion can be seen from Figure 3.

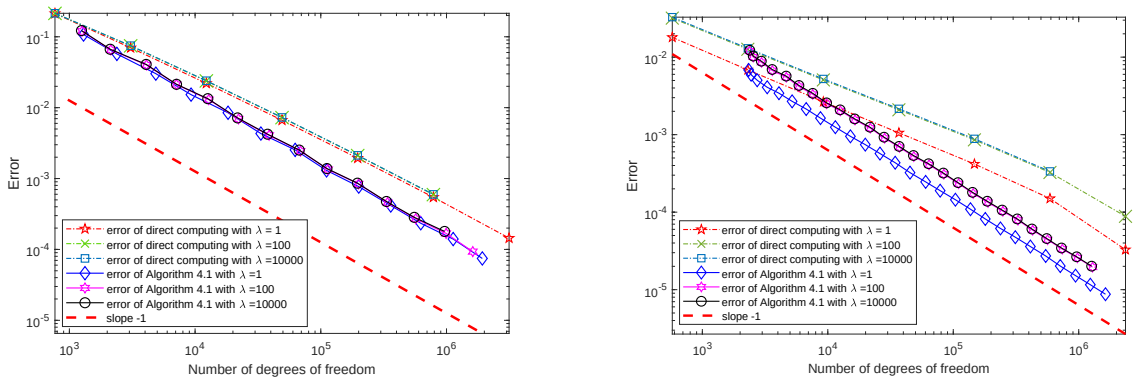

Figure 2. The error curves of directly computing by DGFEM and Algorithm 4.1 by using $P1$ element for the 1st nonzero eigenvalue of (2.3) in Ω_S (left) and Ω_L (right).

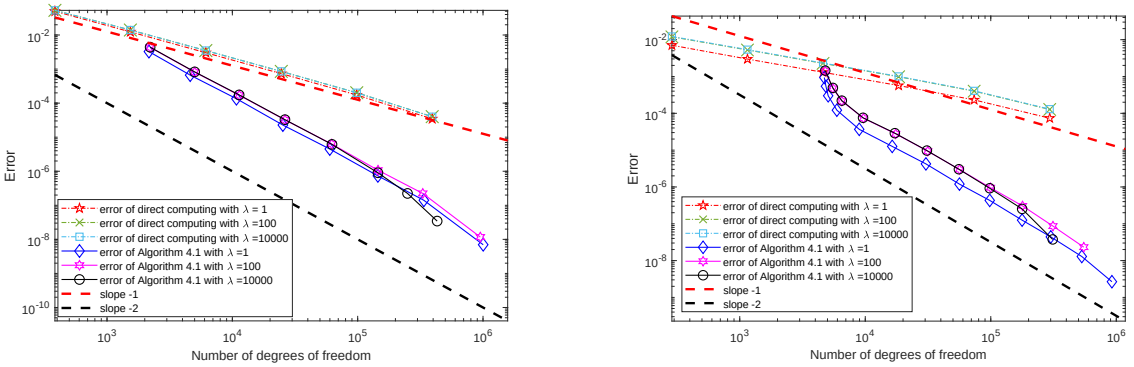

Figure 3. The error curves of directly computing by DGFEM and Algorithm 4.1 by using $P2$ element for the 1st nonzero eigenvalue of (2.3) in Ω_S (left) and Ω_L (right).

Now we use Algorithms 4.1 and 4.2 with $P1$ and $P2$ elements to compute the first 7 non-zero eigenvalues of (2.3) in Ω_S and Ω_L, respectively. When using $P1$ element, the parameters $\mu = 1, \lambda = 1, \gamma_\mu = \gamma_\lambda = 10$ and the diameter of initial mesh is taken as $\frac{\sqrt{2}}{16}$. Limited to space, we list the 1st, the 3rd, the 4th and the 6th approximate eigenvalue in Tables 1 and 2. We also depict the error curves of approximate eigenvalues by Algorithm 4.1 and the curve of error indicators in Figure 4, where the reference values are taken as the most accurate approximations that we can compute. In addition, for the 1st non-zero eigenvalue of (2.3), we investigate the influence of Lamé parameter by taking $\lambda = 1, 10, 100, 1000, 10000$, and the corresponding error curves are shown in Figure 5. When using $P2$ element, the parameters $\mu = \lambda = 1, \gamma_\mu = \gamma_\lambda = 40$ and the diameter of initial mesh is taken as $\frac{\sqrt{2}}{8}$. In Tables 3 and 4 we list the 1st, the 3rd, the 4th and the 6th approximate eigenvalue. We also plot

the error curves of approximate eigenvalues by Algorithm 4.1 and the curve of error indicators in Figure 6. For the 1st non-zero eigenvalue of (2.3), we investigate the influence of Lamé parameter by taking $\lambda = 1, 10, 100, 1000, 10000$, and the corresponding error curves are shown in Figure 7.

Table 1. The results in Ω_S by Algorithms 4.1 and 4.2 with $P1$ element.

j	l	$N_{j,l}$	$\kappa_j^{h_l}$	$CPU_{j,l}(s)$	l	$N_{j,l}$	κ_{j,h_l}	$CPU_{j,l}(s)$
1	1	3600	2.5834151705	0.05433	1	3600	2.5834151539	0.06679
1	8	26328	2.5365029347	1.62136	8	26328	2.5365029348	2.52953
1	21	1208232	2.5310939833	249.69061	21	1208232	2.5310939827	391.04103
1	22	1570164	2.5310583228	485.28739	22	1570164	2.5310583228	651.02095
1	23	2050932	2.5310346038	817.8231911	23	2050932	2.531034604	1167.502765
3	1	3324	2.7404121518	0.02745	1	3324	2.7414582353	0.07244
3	11	30156	2.6778807957	1.75582	16	43908	2.6778901580	7.73674
3	20	428676	2.6740736381	57.92155	31	605400	2.6740696701	244.04938
3	23	1026540	2.6739097335	212.85588	34	1025280	2.6739660124	488.60793
3	24	1349388	2.6738786576	395.09095	35	1219860	2.6739372698	624.67912
4	1	3888	3.7164345114	0.05795	1	3888	3.7164345114	0.10192
4	9	44460	3.7115741607	3.84681	9	44460	3.7115741607	5.61523
4	22	1762944	3.7111432638	194.69801	22	1762944	3.7111432638	341.67732
4	23	2344044	3.7111398968	269.71127	23	2344044	3.7111398969	470.55583
4	24	3028620	3.7111378848	385.01813	24	3028620	3.7111378848	654.91996
6	1	3792	5.2873876626	0.06042	1	3792	5.2873876273	0.09334
6	5	11784	5.2632333578	0.70311	5	11784	5.2632333578	1.11777
6	20	942528	5.2537917257	198.46971	20	942528	5.2537917253	306.96848
6	21	1259328	5.2537597122	334.17056	21	1259328	5.2537597120	452.24058
6	22	1636512	5.2537348070	605.55218	22	1636512	5.2537348072	796.76924

Table 2. The results in Ω_L by Algorithms 4.1 and 4.2 with $P1$ element.

j	l	$N_{j,l}$	$\kappa_j^{h_l}$	$CPU_{j,l}(s)$	l	$N_{j,l}$	κ_{j,h_l}	$CPU_{j,l}(s)$
1	1	9252	1.1578406889	0.08684	1	9252	1.1578406889	0.21686
1	4	9960	1.1568717901	0.51428	4	9960	1.1568717901	1.05144
1	22	854196	1.1551704849	83.61915	22	854520	1.1551704801	143.97265
1	23	1125306	1.1551665423	116.92568	23	1125690	1.1551665389	193.87293
1	24	1469730	1.1551634294	330.33730	24	1470228	1.1551634258	431.50241
3	1	9852	2.0253499592	0.10770	1	9852	2.0253499590	0.24006
3	3	13236	2.0200276681	0.62807	3	13236	2.0200276680	1.21075
3	18	1072320	2.0137654513	221.81309	18	1072320	2.0137654513	344.53795
3	19	1431672	2.0137487824	351.63554	19	1431672	2.0137487822	590.05031
3	20	1924536	2.0137351315	711.94221	20	1924536	2.0137351315	1029.63061
4	1	9540	2.1396949065	0.10559	1	9540	2.1396949061	0.23500
4	4	13446	2.1322409848	0.70466	4	13446	2.1322409847	1.33492
4	19	823536	2.1258417612	147.60184	19	823536	2.1258417612	260.40436
4	20	1085094	2.1258166076	225.83332	20	1085094	2.1258166075	386.16427
4	21	1437324	2.1257991175	324.24898	21	1437324	2.1257991172	566.48046
6	1	9828	2.7939491213	0.15553	1	9828	2.7939490858	0.31958
6	3	12894	2.7668920157	0.78224	3	12894	2.7668920151	1.00058
6	18	965010	2.7367899041	163.71460	18	965010	2.7367899035	335.07813
6	19	1292184	2.7367099740	271.08934	19	1292184	2.7367099727	503.74878
6	20	1729368	2.7366439994	494.77192	20	1729368	2.7366439984	797.84910

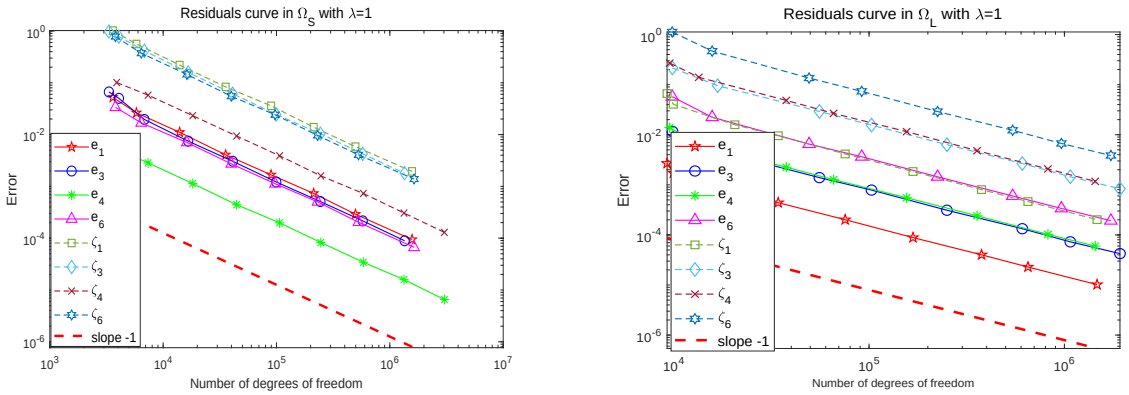

Figure 4. Convergence study of Algorithm 4.1 by $P1$ element in Ω_S (left) and Ω_L (right).

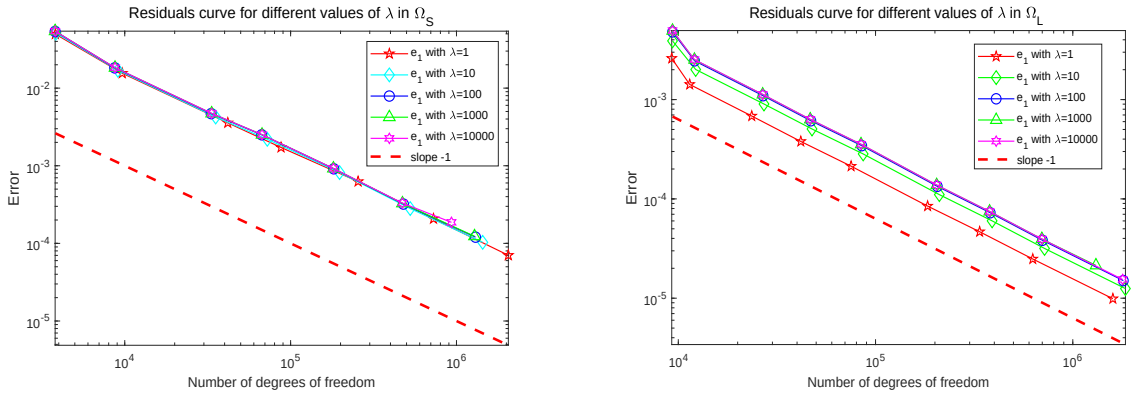

Figure 5. Robustness study of Algorithm 4.1 by $P1$ element in Ω_S (left) and Ω_L (right).

Table 3. The results in Ω_S by Algorithms 4.1 and 4.2 with $P2$ element.

j	l	$N_{j,l}$	$\kappa_j^{h_l}$	$CPU_{j,l}(s)$	l	$N_{j,l}$	κ_{j,h_l}	$CPU_{j,l}(s)$
1	1	1632	2.5399573563	0.20754	1	1632	2.5399573531	0.33385
1	5	3600	2.5321126514	0.80285	5	3600	2.5321126514	1.16189
1	24	760152	2.5309641786	211.46084	24	760152	2.5309641786	239.26807
1	25	1003368	2.5309641677	278.22507	25	1003368	2.5309641677	320.01464
1	26	1339404	2.5309641607	378.58015	26	1339404	2.5309641607	439.05795
3	1	1584	2.6862908794	0.12511	1	1584	2.6862921826	0.40313
3	18	43920	2.6737990072	8.60574	24	46896	2.6737995054	17.94984
3	30	813360	2.6737894142	210.84097	42	823224	2.6737894180	409.26749
3	31	1021272	2.6737894039	275.45868	44	1129272	2.6737894027	587.31383
3	32	1276776	2.6737893962	363.84821	45	1328904	2.6737893981	708.17810
4	1	1824	3.7114311740	0.13369	1	1824	3.7114311740	0.21961
4	5	6360	3.7111583273	0.89324	5	6360	3.7111583273	1.89695
4	22	754512	3.7111313470	178.28979	22	754512	3.7111313471	250.31766
4	23	939408	3.7111313465	244.08245	23	939408	3.7111313466	341.16368
4	24	1218768	3.7111313461	339.61412	24	1218768	3.7111313462	460.76539
6	2	1920	5.2557235447	0.49529	2	1920	5.2557235444	0.59788
6	8	8904	5.2537750836	1.87161	8	8904	5.2537750836	2.28091
6	24	838920	5.2536682063	197.38184	24	838920	5.2536682064	267.40500
6	25	1119096	5.2536682008	270.08041	25	1119096	5.2536682009	376.06184
6	26	1456968	5.2536681969	380.87500	26	1456968	5.2536681971	520.85769

Table 4. The results in Ω_L by Algorithms 4.1 and 4.2 with $P2$ element.

j	l	$N_{j,l}$	$\kappa_j^{h_l}$	$CPU_{j,l}(s)$	l	$N_{j,l}$	κ_{j,h_l}	$CPU_{j,l}(s)$
1	1	4656	1.1562458918	0.38986	1	4656	1.1562458918	0.55317
1	25	66996	1.1551541513	18.31403	25	66996	1.1551541513	22.07079
1	38	774480	1.1551532609	260.06329	38	774480	1.1551532609	325.52552
1	39	923052	1.1551532590	320.61556	39	923052	1.1551532591	400.40419
1	40	1099044	1.1551532576	398.76151	40	1099044	1.1551532576	496.73607
3	1	4680	2.0159225406	0.46936	1	4680	2.0159225405	0.57221
3	9	19224	2.0137381688	4.00481	9	19224	2.0137381688	5.20982
3	23	976428	2.0136927626	233.96942	23	976428	2.0136927626	313.17266
3	24	1280052	2.0136927550	324.92148	24	1280052	2.0136927550	421.48383
3	25	1679592	2.0136927505	458.31975	25	1679592	2.0136927505	578.37647
4	10	11316	2.1259084959	3.98294	10	11316	2.1259084959	4.01302
4	21	105648	2.1257416544	27.89323	21	105648	2.1257416544	37.43586
4	32	822120	2.1257391878	297.07841	32	822120	2.1257391878	368.95873
4	33	980688	2.1257391755	362.49125	33	980688	2.1257391755	456.94719
4	34	1181328	2.1257391658	446.73985	34	1181328	2.1257391658	572.04947
6	1	4680	2.7468959498	0.40303	1	4680	2.7468959503	0.61874
6	3	5232	2.7405213916	0.92105	3	5232	2.7405213907	1.21365
6	23	1000704	2.7364519542	234.72412	23	1000704	2.7364519542	334.60146
6	24	1312716	2.7364519227	327.39089	24	1312716	2.7364519227	448.35877
6	25	1726080	2.7364519037	468.01995	25	1726080	2.7364519038	608.05296

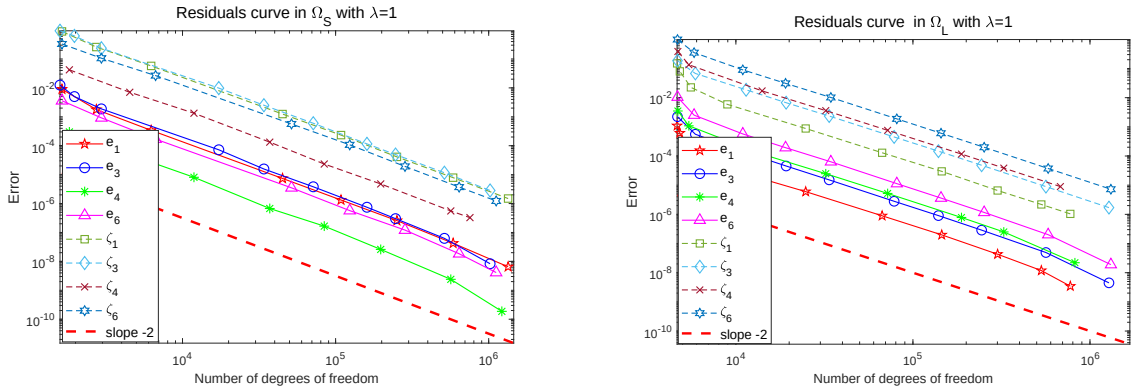

Figure 6. Convergence study of Algorithm 4.1 by $P2$ element in Ω_S (left) and Ω_L (right).

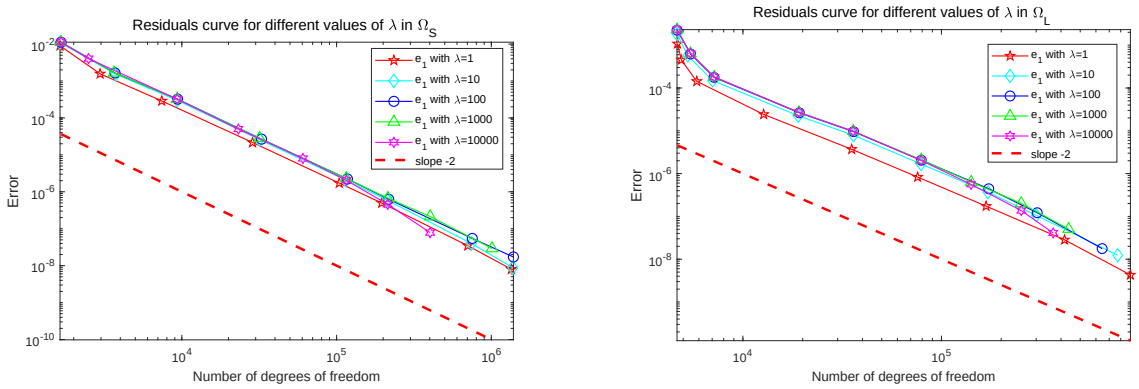

Figure 7. Robustness study of Algorithm 4.1 by $P2$ element in Ω_S (left) and Ω_L (right).

It can be seen from Tables 1–4 that to get the same accurate approximate eigenvalues, Algorithm 4.1 uses less time or less degrees of freedom than Algorithm 4.2. In Figure 4, the error curves e_1, e_3, e_4 and e_6 are all parallel to the line with slope -1, and in Figure 6 the error curves e_1, e_3, e_4 and e_6 are parallel to the line with slope -2, which indicate that the approximate eigenvalues obtained by Algorithm 4.1 achieve the optimal convergence order. Meanwhile, in Figure 5, the error curves e_1, e_3, e_4 and e_6 are almost parallel to the curve of $\zeta_1, \zeta_3, \zeta_4$ and ζ_6 respectively, and in Figure 7, the curves of e_1, e_3, e_4 and e_6 are parallel to $\zeta_1, \zeta_3, \zeta_4$ and ζ_6, which indicate that the error indicators are reliable and efficient. Figures 5 and 7 then show that Algorithm 4.1 is robust in both Ω_S and Ω_L.

5. Conclusions

In this paper, we discussed a multigrid discretization scheme of DGFEM based on the shifted-inverse iteration. Theoretical analysis and numerical results all showed that this method can efficiently solve the Steklov-Lamé eigenproblem as we expected. Generally, the time of solving a linear algebraic system is much less than that of solving an eigenvalue problem. Further, we observe from Tables 1–4 that although the CPU time of the adaptive DG-multigrid method is less than that of the standard adaptive DGFEM, the advantage is not obvious. We think that this may be because we use "\" to solve linear algebraic systems. We notice that in recent research, the multigrid method has been combined with other methods to form many efficient algorithms and applied to many problems, as combined with the DG method in this paper. For example, the multigrid-homotopy method to diffusion equation [42], the multigrid method for the semilinear interface problem based on the modified two-grid method [43], the multigrid method for nonlinear eigenvalue problems based on Newton iteration [44], etc. It is of interest for us to explore more applications of multigrid methods and more efficient solvers for solving linear algebraic equations in multigrid methods.

Acknowledgments

This work was supported by the National Natural Science Foundation of China (No. 12261024) and Science and Technology Planning Project of Guizhou Province (Guizhou Kehe fundamental research-ZK[2022] No.324).

Conflict of interest

This work does not have any conflicts of interest.

References

1. A. Girouard, I. Polterovich, Spectral geometry of the Steklov problem, *J. Spectr. Theory*, **7** (2017), 321–360. https://doi.org/10.4171/JST/164
2. M. Levitin, P. Monk, V. Selgas, Impedance eigenvalues in linear elasticity, *SIAM J. Appl. Math.*, **81** (2021), 2433–2456. https://doi.org/10.1137/21M1412955
3. F. Magoulès, F. X. Roux, L. Series, Algebraic approximation of Dirichlet-to-Neumann maps for the equations of linear elasticity, *Comput. Methods Appl. Mech. Eng.*, **195** (2006), 3742–3759. https://doi.org/10.1016/j.cma.2005.01.022
4. F. Magoulès, F. X. Roux, L. Series, Algebraic Dirichlet-to-Neumann mapping for linear elasticity problems with extreme contrasts in the coefficients, *Appl. Math. Model.*, **30** (2006), 702–713. https://doi.org/10.1016/j.apm.2005.07.008
5. S. Domínguez, Steklov eigenvalues for the Lamé operator in linear elasticity, *J. Comput. Appl. Math.*, **394** (2021), 113558. http://doi.org/10.1016/J.CAM.2021.113558
6. Y. Li, H. Bi, A locking-free discontinuous Galerkin method for linear elastic Steklov eigenvalue problem, *Appl. Numer. Math.*, **188** (2023), 21–41. https://doi.org/10.1016/j.apnum.2023.02.018
7. I. Babuška, M. Suri, Locking effects in the finite element approximation of elasticity problems, *Numer. Math.*, **62** (1992), 439–463. http://doi.org/10.1007/bf01396238
8. I. Babuška, M. Suri, On locking and robustness in the finite element method, *SIAM J. Numer. Anal.*, **29** (1992), 1261–1293. http://doi.org/10.1137/0729075
9. M. Vogelius, An analysis of the p-version of the finite element method for nearly incompressible materials, *Numer. Math.*, **41** (1983), 39–53. https://doi.org/10.1007/BF01396304
10. D. N. Arnold, F. Brezzi, J. Douglas, PEERS: A new mixed finite element for plane elasticity, *Japan J. Appl. Math.*, **1** (1984), 347–367. http://doi.org/10.1007/bf03167064
11. R. Stenberg, A family of mixed finite elements for the elasticity problem, *Numer. Math.*, **53** (1988), 513–538. https://doi.org/10.1007/bf01397550
12. L. Franca, R. Stenberg, Error analysis of some Galerkin-least-squares methods for the elasticity equations, *SIAM J. Numer. Anal.*, **28** (1991), 1680–1697. http://www.jstor.org/stable/2157955
13. R. S. Falk, Nonconforming finite element methods for the equations of linear elasticity, *Math. Comput.*, **57** (1991), 529–550. http://doi.org/10.1090/s0025-5718-1991-1094947-6
14. S. C. Brenner, L. Y. Sung, Linear finite element methods for planar linear elasticity, *Math. Comput.*, **59** (1992), 321–338. http://doi.org/10.1090/s0025-5718-1992-1140646-2
15. T. P. Wihler, Locking-free DGFEM for elasticity problems in polygons, *IMA J. Numer. Anal.*, **24** (2004), 45–75. https://doi.org/10.1093/imanum/24.1.45
16. T. P. Wihler, Locking-free adaptive discontinuous Galerkin FEM for linear elasticity problems, *Math. Comput.*, **75** (2006), 1087–1102. https://doi.org/10.2307/4100266

17. T. Steiner, P. Wriggers, S. Loehnert, A discontinuous Galerkin finite element method for linear elasticity using a mixed integration scheme to circumvent shear-locking, *PAMM*, **16** (2016), 769–770. https://doi.org/10.1002/pamm.201610373

18. J. Xu, A. Zhou, A two-grid discretization scheme for eigenvalue problems, *Math. Comput.*, **70** (1999), 17–25. https://doi.org/10.2307/2698923

19. J. Xu, A. Zhou, Local and parallel finite element algorithms for eigenvalue problems, *Acta. Math. Appl. Sin.*, **18** (2002), 185–200. https://doi.org/10.1007/s102550200018

20. Y. Yang, H. Bi, Two-grid finite element discretization schemes based on shifted-inverse power method for elliptic eigenvalue problems, *SIAM J. Numer. Anal.*, **49** (2011), 1602–1624. https://doi.org/10.1137/100810241

21. Q. Li, Y. Yang, A two-grid discretization scheme for the Steklov eigenvalue problem, *J. Appl. Math. Comput.*, **36** (2011), 129–139. https://doi.org/10.1007/s12190-010-0392-9

22. H. Bi, Y. Yang, A two-grid method of the non-conforming Crouzeix-Raviart element for the Steklov eigenvalue problem, *Appl. Math. Comput.*, **217** (2011), 9669–9678. http://doi.org/10.1016/j.amc.2011.04.051

23. M. Xie, F. Xu, M. Yue, A type of full multigrid method for non-selfadjoint Steklov eigenvalue problems in inverse scattering, *ESAIM Math. Model. Numer. Anal.*, **55** (2021), 1779–1802. https://doi.org/10.1051/m2an/2021039

24. M. Yue, F. Xu, M. Xie, A multilevel Newton's method for the Steklov eigenvalue problem, *Adv. Comput. Math.*, **48** (2022), 33. https://doi.org/10.1007/s10444-022-09934-6

25. A. Andreev, R. Lazarov, M. Racheva, Postprocessing and higher order convergence of the mixed finite element approximations of biharmonic eigenvalue problems, *J. Comput. Appl. Math.*, **182** (2005), 333–349. http://doi.org/10.1016/j.cam.2004.12.015

26. C. S. Chien, B. W. Jeng, A two-grid discretization scheme for semilinear elliptic eigenvalue problems, *SIAM J. Sci. Comput.*, **27** (2006), 1287–1304. http://doi.org/10.1137/030602447

27. X. Dai, A. Zhou, Three-scale finite element discretizations for quantum eigenvalue problems, *SIAM J. Numer. Anal.*, **46** (2008), 295–324. http://doi.org/10.1137/06067780x

28. H. Chen, S. Jia, H. Xie, Postprocessing and higher order convergence for the mixed finite element approximations of the Stokes eigenvalue problems, *Appl. Math.*, **54** (2009), 237–250. http://doi.org/10.1007/s10492-009-0015-7

29. H. Xie, X. Yin, Acceleration of stabilized finite element discretizations for the Stokes eigenvalue problem, *Adv. Comput. Math.*, **41** (2015), 799–812. https://doi.org/10.1007/s10444-014-9386-8

30. J. Chen, Y. Xu, J. Zou, An adaptive inverse iteration for Maxwell eigenvalue problem based on edge elements, *J. Comput. Phys.*, **229** (2010), 2649–2658. http://doi.org/10.1016/j.jcp.2009.12.013

31. M. R. Racheva, A. B. Andreev, Superconvergence postprocessing for eigenvalues, *Comp. Methods Appl. Math.*, **2** (2002), 171–185. https://doi.org/10.2478/cmam-2002-0011

32. Y. Yang, H. Bi, J. Han, Y. Yu, The shifted-inverse iteration based on the multigrid discretizations for eigenvalue problems, *SIAM J. Sci. Comput.*, **37** (2015), A2583–A2606. https://doi.org/10.1137/140992011

33. P. Hansbo, M. G. Larson, Discontinuous Galerkin methods for incompressible and nearly incompressible elasticity by Nitsche's method, *Comput. Methods Appl. Mech. Eng.*, **191** (2002), 1895–1908. http://doi.org/10.1016/s0045-7825(01)00358-9

34. I. Babuška, J. E. Osborn, Eigenvalue Problems, In: *Finite Element Methods (Part I)*, North-Holand: Elsevier Science Publishers, 641–787, 1991.

35. L. Chen, *An Integrated Finite Element Method Package in MATLAB*, California: University of California at Irvine, 2009.

36. L. N. Trefethen, D. Bau, *Numerical Linear Algebra*, Philadelphia: SIAM, 1997.

37. P. Hansbo, M. G. Larson, Energy norm a posteriori error estimates for discontinuous Galerkin approximations of the linear elasticity problem, *Comput. Methods Appl. Mech. Engrg.*, **200** (2011), 3026–3030. http://doi.org/10.1016/j.cma.2011.06.008

38. W. Dörfler, A convergent adaptive algorithm for Poisson's equation, *SIAM J. Numer. Anal.*, **33** (1996), 1106–1124. http://doi.org/10.2307/2158497

39. J. M. Maubach, Local bisection refinement for n-simplicial grids generated by reflection, *SIAM J. Sci. Comput.*, **16** (1995), 210–227. https://doi.org/10.1137/0916014

40. P. Morin, R. H. Nochetto, K. Siebert, Data oscillation and convergence of adaptive FEM, *SIAM J. Numer. Anal.*, **38** (2000), 466–488. https://doi.org/10.2307/3062065

41. X. Dai, J. Xu, A. Zhou, Convergence and optimal complexity of adaptive finite element eigenvalue computations, *Numer. Math.*, **110** (2008), 313–355. http://doi.org/10.1007/s00211-008-0169-3

42. T. Liu, Parameter estimation with the multigrid-homotopy method for a nonlinear diffusion equation, *J. Comput. Appl. Math.*, **413** (2022), 114393. https://doi.org/10.1016/j.cam.2022.114393

43. F. Xu, Y. Guo, Q. Huang, H. Ma, An efficient multigrid method for semilinear interface problems, *Appl. Numer. Math.*, **179** (2022), 238–254. https://doi.org/10.1016/j.apnum.2022.05.003

44. F. Xu, M. Xie, M. Yue, Multigrid method for nonlinear eigenvalue problems based on Newton iteration, *J. Sci. Comput.*, **94** (2023), 42. https://doi.org/10.1007/s10915-022-02070-9

AIMS Press